Journal of Medicinal Chemistry

Article

pubs.acs.org/jmc

Imidazolopiperazines: Lead Optimization of the Second-Generation Antimalarial Agents

Advait Nagle,[†,#] Tao Wu,[†,#] Kelli Kuhen,[†] Kerstin Gagaring,[†] Rachel Borboa,[†] Caroline Francek,[†] Zhong Chen,[†] David Plouffe,[†] Xuena Lin,[‡] Christopher Caldwell,[‡] Jared Ek,[†] Suzanne Skolnik,[‡] Fenghua Liu,[‡] Jianling Wang,[‡] Jonathan Chang,[†] Chun Li,[†] Bo Liu,[†] Thomas Hollenbeck,[†] Tove Tuntland,[†] John Isbell,[†] Tiffany Chuan,[†] Philip B. Alper,[†] Christoph Fischli,[§,∥] Reto Brun,[§,∥] Suresh B. Lakshminarayana,[⊥] Matthias Rottmann,[§,∥] Thierry T. Diagana,[⊥] Elizabeth A. Winzeler,[†] Richard Glynne,[†] David C. Tully,[†] and Arnab K. Chatterjee*[,†]

[†]Genomics Institute of the Novartis Research Foundation, 10675 John Jay Hopkins Drive, San Diego, California 92121, United States

[‡]Novartis Institute for Biomedical Research, Preclinical Profiling Group, Cambridge, Massachusetts

[§]Swiss Tropical and Public Health Institute, Parasite Chemotherapy, CH-4002 Socinstrasse 57, CD-4002 Basel, Switzerland

[∥]University of Basel, CH-4003 Basel, Switzerland

[⊥]Novartis Institute for Tropical Diseases, 10 Biopolis Road, 05-01 Chromos, Singapore-138670

Supporting Information

ABSTRACT: On the basis of the initial success of optimization of a novel series of imidazolopiperazines, a second generation of compounds involving changes in the core piperazine ring was synthesized to improve antimalarial properties. These changes were carried out to further improve the potency and metabolic stability of the compounds by leveraging the outcome of a set of in vitro metabolic identification studies. The optimized 8,8-dimethyl imidazolopiperazine analogues exhibited improved potency, in vitro metabolic stability profile and, as a result, enhanced oral exposure in vivo in mice. The optimized compounds were found to be more efficacious than the current antimalarials in a malaria mouse model. They exhibit moderate oral exposure in rat pharmacokinetic studies to achieve sufficient multiples of the oral exposure at the efficacious dose in toxicology studies.

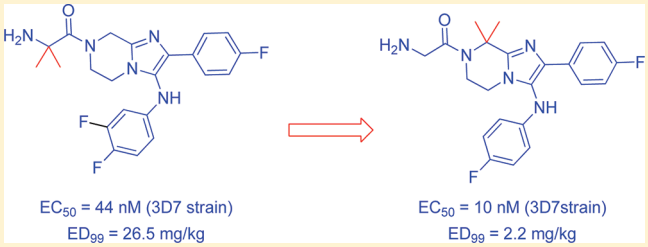

INTRODUCTION

After decades of neglect, the search for novel, effective antimalarials has been revived primarily due to emergence of drug resistance.[1] Widespread resistance has been reported not only for 8-aminoquinolines but recent reports indicate the appearance of increased parasite tolerance to artemisinin analogues, potentially predicating clinical resistance.[2] The absence of highly efficacious malaria vaccines highlights the importance of developing small-molecule drugs.[3] With support from the Wellcome Trust and Medicines for Malaria Venture (MMV), the NGBS consortium (the Novartis Institute for Tropical Diseases (NITD), the Genomics Institute of the Novartis Research Foundation (GNF), the Biomedical Primate Research Centre (BPRC), and the Swiss Tropical and Public Health Institute (STPHI)) was formed and set up to discover new antimalarials which are effective against multidrug resistant parasite strains. This collaboration has produced promising new leads.[1a,4] Here we report our continued effort to optimize a series of imidazolopiperazine compounds in search of a preclinical candidate. The lead compound we identified was compound **1**.[5] As described previously, an extensive SAR study on the three peripheral parts had yielded decent in vitro and in vivo antimalarial activities as well as favorable physiochemical and pharmacokinetic properties.

Our efforts toward the first-generation compounds led to candidates (like compound **1**) with double-digit nanomolar potency and moderate oral exposure in mice. However, most potent compounds with an unsubstituted piperazine had poor oral exposure which resulted in inferior in vivo efficacy when administered orally, for example, compounds **28** and **31** (Scheme 1) in the previous communication (Figure 1).[5] We were intrigued by the possibility of further refining the core structure of the molecule to further improve the properties. Our hypothesis was further reinforced by chemical stability and mouse in vitro metabolic stability results which led to the identification of two biologically inactive metabolites (**1a** and **1b**) arising from the oxidation of piperazine ring. Our plan was to substitute three possible positions (positions 5, 6, and 8) to

Received: January 11, 2012
Published: April 23, 2012

Scheme 1. Unsubstituted Piperazines Previously Disclosed

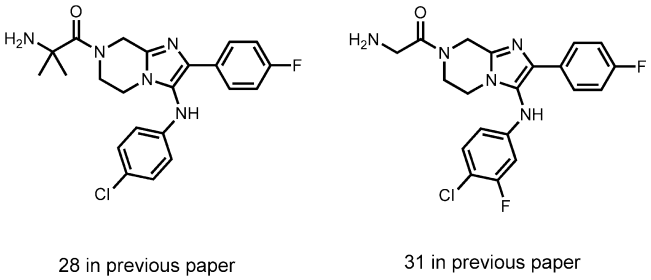

evaluate the corresponding effects on potency as well as a means to improve oral exposure.

CHEMISTRY

On the basis of the designed molecules, it was clear that previous synthetic routes were not amenable for the desired compounds because we could not utilize the 3 + 2 cyclization.[6] Distinct syntheses were designed and executed to obtain substitution at different positions of a piperazine ring. Scheme 2 summarizes how the 8-substituted piperazines were prepared. The synthesis started with an alkylation reaction between Cbz-protected glycine derivative **2** and bromide **3**. Adduct **4** was then refluxed with NH_4OAc in toluene to give imidazole **5** with removal of water using a Dean−Stark apparatus.[7] Regioselective *N*-alkylation with ethyl 2-bromoacetate followed by a one-pot deprotection/cyclization sequence furnished the lactam core, which was reduced by borane to furnish amine **8**. The quaternary *β*-carbon did not pose a significant amount of steric hindrance for the HATU mediated amidation reaction with *N*-Boc-glycine. Amide **9** was obtained at room temperature in decent yield and further was brominated to provide intermediate **10**. Then a standard Buchwald−Hartwig amination reaction with substituted aniline followed by deprotection finished the synthesis of compound **12** with the desired alkyl modification at position 8. The overall sequence involved nine steps with an overall yield of 17%.

Scheme 3 describes the synthesis of 6,6-dimethyl analogues. Analogous chemistry to compound **12** was used for the first two steps to provide imidazole **5a**. The compound was regioselectively *N*-alkylated with methallyl chloride to obtain the key intermediate for the piperazine cyclization step. The intramolecular hydroamination reaction proved to be difficult, and after extensive screening, treating the substrate **5a** with a 5:1 mixture of acetic acid and methanesulfonic acid at 210 °C produced the cyclized core with simultaneous loss of the

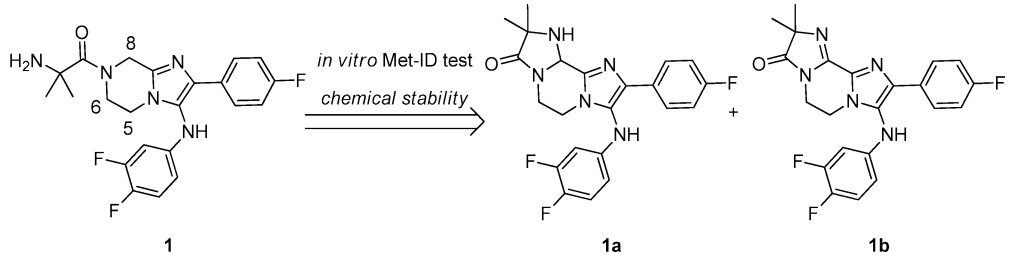

Figure 1. Central piperazine ring oxidation is a major metabolic and chemical instability site in compound **1**.

Scheme 2. Modification on the 8 Position of Imidazolopiperazine Core[a]

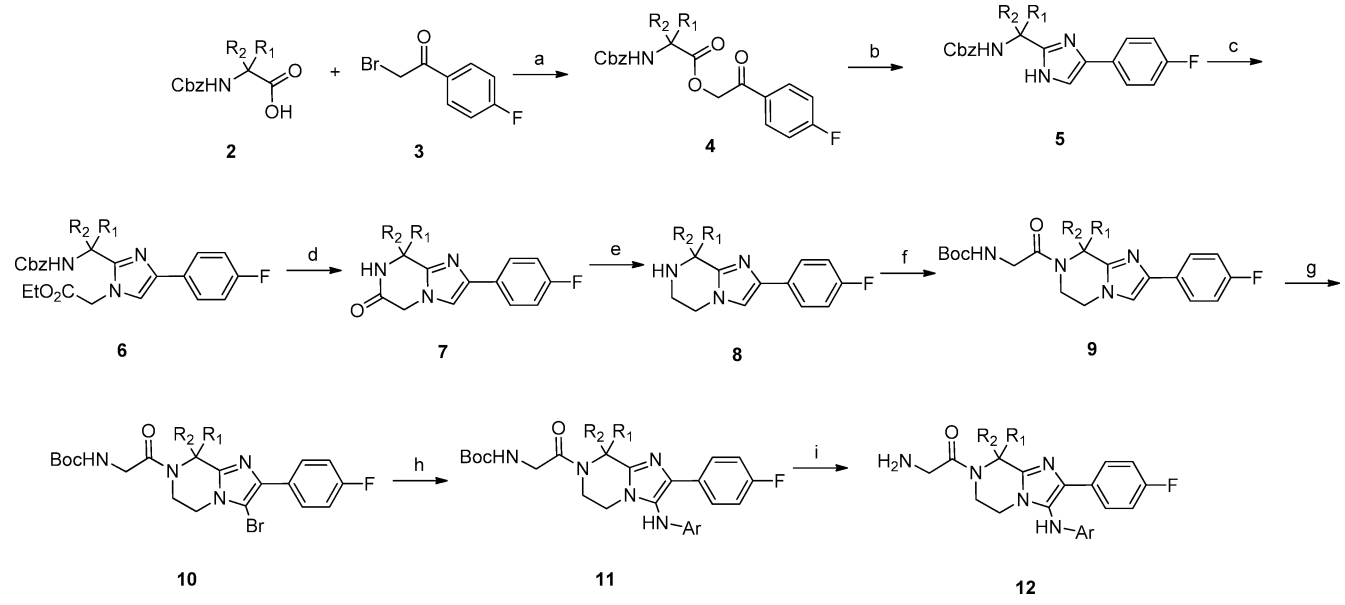

[a]Reagents and conditions: (a) K_2CO_3, DMF, rt, 84%; (b) NH_4OAc, toluene, reflux, 88% (c) ethyl 2-bromoacetate, Cs_2CO_3, DMF, rt, 83%; (d) Pd/C, H_2 (balloon), MeOH, rt, 91%; (e) BH_3·THF, THF, reflux, 95%; (f) HATU, DIEA, CH_2Cl_2, rt, 70%; (g) Br_2, AcOH, CH_2Cl_2, rt, 100%; (h) $ArNH_2$, $Pd_2(dba)_3$, xantphos, Cs_2CO_3, dioxane, 150 °C, 89% (for example **22**, Ar = 4F-Ph and $R_1 = R_2$ = Me); (i) TFA, CH_2Cl_2, rt, 52% (for example **22**, Ar = 4F-Ph and $R_1 = R_2$ = Me).

dx.doi.org/10.1021/jm300041e | J. Med. Chem. 2012, 55, 4244−4273

Scheme 3. Modification on the 6 Position of Imidazolopiperazine Core[a]

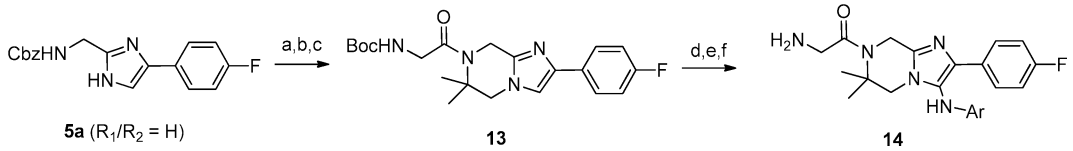

[a]Reagents and conditions: (a) methallyl chloride, K_2CO_3, KI, DMF, rt, 55%; (b) AcOH/MsOH (6:1), 210 °C, 39%; (c) *N*-Boc-glycine, HATU, DIEA, DMF, rt; 57%; (d) Br_2, AcOH, CH_2Cl_2, rt; 55%; (e) $ArNH_2$, $Pd_2(dba)_3$, xantphos, Cs_2CO_3, dioxane, 150 °C; (f) TFA, CH_2Cl_2, rt, 55% over 2 steps (for example **25**, Ar = 4F-Ph).

Scheme 4. Modification on the 5 Position of Imidazolopiperazine Core[a]

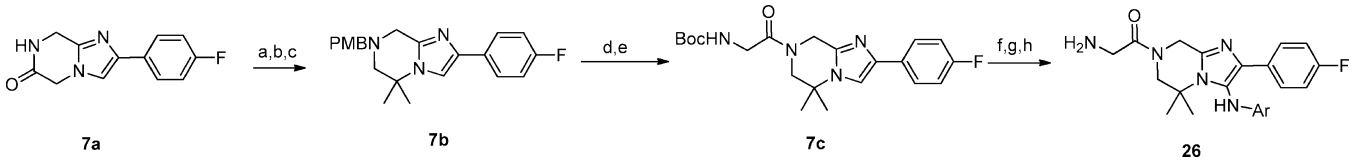

[a]Reagents and conditions: (a) PMBCl, KOH, DMF, 0 °C to rt, 63%; (b) MeI, NaH, DMF, rt, 86%; (c) BH_3·THF, THF, reflux, 100%; (d) TFA, 70 °C, quantitative; (e) *N*-Boc-glycine, HATU, TEA, DMF, rt, 49%; (f) Br_2, AcOH, CH_2Cl_2, 90%; (g) $ArNH_2$, $Pd_2(dba)_3$, xantphos, Cs_2CO_3, dioxane, 150 °C; (h) TFA, CH_2Cl_2, rt, 46% over 2 steps for example **26** where Ar = 4F-Ph.

carbamate protecting group. Despite the harsh reaction condition, an acceptable yield of the product (39%) was obtained and the regiochemistry was confirmed by 2D NMR of the intermediate. The cyclized core was subjected to amide coupling with *N*-Boc glycine to yield intermediate **13**. The final steps in the sequence are analogous to Scheme 2 to furnish analogue **14**. The sequence involved six steps from intermediate **5a** with an overall yield of 3.7%. The synthesis of the 5,5-dimethyl modified analogues diverged from their 8,8-dimethyl modified counterparts at intermediate **7a**. *N*-PMB protection was necessary for lactam **7a** before the NaH-mediated bis-methylation at the 5-position (Scheme 4). The lactam was then reduced using borane THF complex to afford **7b**. The bicyclic intermediate was then deprotected and amine was subjected to a HATU mediated amidation to obtain compound **7c**. The final sequence involved bromination followed by palladium-catalyzed aniline amination and Boc-deprotection to furnish 5,5-dimethyl modified compound **26**. The sequence involved eight steps from intermediate **7a** with an overall yield of 10.9%.

RESULTS AND DISCUSSION

Structure–Activity Relationship. We began exploring the SAR on the piperazine ring by substituting at the 8-position first, and we decided to use 4-F-aniline and 3-F-4-Cl aniline based on our previous work at the R_6 position (Table 1).[5] Adding a methyl group to the 8-position led to loss of potency by 10-fold (cmpd **17**), but the compound was still equipotent to compound **15** (Scheme 5). Moreover, there was no profound effect on the potency by changing the absolute configuration of the methyl group. Increasing the size of substituent to isopropyl group led to dramatic loss in potency (examples **19** and **20**). A dimethyl group on the 8-postion not only led to more favorable compound in terms of completely blocking the benzylic carbon as indicated by our metabolite studies but also removing the stereogenic carbon. Surprisingly, substitution of 3Cl-4F aniline in the 8-disubstitution case provided a less potent compound when compared to other anilines (**21** vs **22**, **23**, or **24**).

Emboldened by the increase in the potency based on the substitution on the 8-position, we decided to study the effect of diMe group on the ethylene carbons of the piperazine ring. On the basis of examples **25** and **26**, it was abundantly clear that the dimethyl group on the 8-position had the most significant positive effect on potency. The substitution on the other positions of the piperazine ring only provided modest potencies when compared to 8-substitution, with activities in the double-digit nanomolar range. As the 5-substituted compounds and the 6-substituted compounds were less potent, we decided to focus our attention on the effect of the amide substituent of the piperazine nitrogen with the 8,8-dimethyl group constant. Our previous efforts demonstrated that dimethyl glycine had slightly inferior potency but offered superior oral exposure. In the case of the substituted piperazines, installation of α methylalanine amide provided equipotent compounds (**15** vs **27**, **22** vs **28**, and **23** vs **29**). We proceeded to further understand the overall effect of the dimethylpiperazine on the minimal pharmacophore.

After studying the effects of various substitutions on the piperazine ring and obtaining a significant improvement in activity, we decided to reconfirm the minimal pharmacophore needed for antiplasmodial activity. On the basis of the earlier results, we were able to achieve antiplasmodial activity with EC_{50} in ~160–400 nM range for the core devoid of the amino acid substituent on the piperazine nitrogen (compound **31**, Table 2). Modification of the piperazine ring into the corresponding lactam led to a ~7-fold decrease in activity in the micromolar range (**32**). However, the antiplasmodial activity is regained by introduction of dimethyl substituent on the 8-position with a 7-fold improvement (**33**). The most optimal compound from this lactam subseries was a compound with 3Cl-4F aniline substitution with an activity around 50–100 nM (**34**). The dimethyl substitution on the reduced piperazine core led to ~10-fold improvement in potency (**31** vs **35**) with compounds to ~10 nM range. These results led us to conclude that the amino acid substitution had minimal to no effect on the potency of the compound with substitution on the 8-position of the imidazolopiperazine core and that the basicity

dx.doi.org/10.1021/jm300041e | J. Med. Chem. 2012, 55, 4244–4273

Table 1. SAR Study for Analogues with Substitution on the Piperazine Core[a]

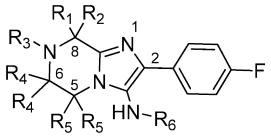

							P. falciparum strain EC_{50}	
compd	R_1	R_2	R_3	R_4	R_5	R_6	3D7 (nM)	W2 (nM)
15	H	H	gly	H	H	4-FPh	24 ± 2	23 ± 8
16	H	H	gly	H	H	3Cl,4F-Ph	4 ± 3	4 ± 2
17	(*S*)-Me	H	gly	H	H	3Cl,4F-Ph	29 ± 2	24 ± 1
18	(*R*)-Me	H	gly	H	H	3Cl,4F-Ph	31 ± 4	29 ± 3
19	(*S*)-*i*-Pr	H	gly	H	H	3Cl,4F-Ph	343 ± 59	470 ± 130
20	(*R*)-*i*-Pr	H	gly	H	H	3Cl,4F-Ph	168 ± 15	202 ± 38
21	Me	Me	gly	H	H	3Cl,4F-Ph	27 ± 1	24 ± 1
22	Me	Me	gly	H	H	4-FPh	10 ± 3	6 ± 1
23	Me	Me	gly	H	H	4-MePh	8 ± 2	6 ± 1
24	Me	Me	gly	H	H	3,4-diFPh	4 ± 1	5 ± 1
25	H	H	gly	Me	H	4-FPh	82 ± 7	111 ± 17
26	H	H	gly	H	Me	4-FPh	80 ± 5	76 ± 15
27	H	H	α-Me-Ala	H	H	4-FPh	20 ± 5	25 ± 2
28	Me	Me	α-Me-Ala	H	H	4-FPh	10 ± 1	9 ± 1
29	Me	Me	α-Me-Ala	H	H	4-MePh	2 ± 1	4 ± 1
30	Me	Me	α-Me-Ala	H	H	3,4-diFPh	13 ± 3	7 ± 1

[a]Values are means of two experiments. Each assay plate has mefloquine, sulfadoxine, and artimesinin as internal standards. The EC_{50} values for standard compounds match the literature values.

Scheme 5. Structures of Key Compounds

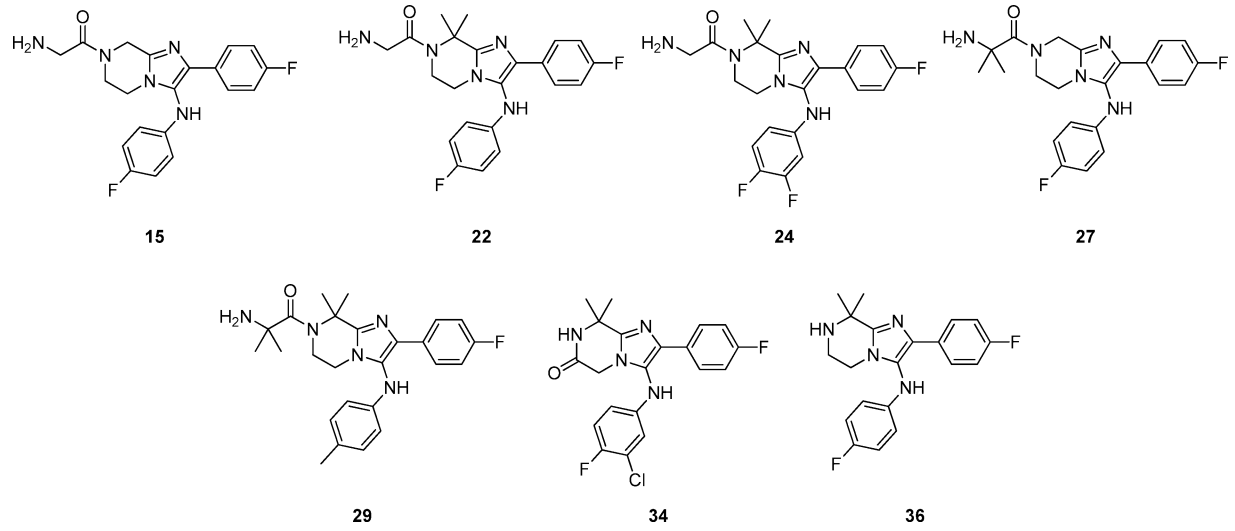

of the piperazine nitrogen could be modulated without complete loss in antimalarial activity.

ADME and Pharmacokinetic Properties. In parallel to the SAR studies to optimize the potency of the compounds series, we evaluated the in vitro ADME and in vivo pharmacokinetic properties of key analogues. In general, this series of compounds had very good Lipinski's rule-of-five compliance and most of the analogues were highly soluble (>175 μM at pH 6.8), with the neutral lactams being least soluble among all the compounds. Table 3 summarizes the in vitro ADME profiles of the important compounds. Typically, a range of values in the permeability assays was observed. In the Caco-2 assays, the core piperazine compounds (both lactams as well as nonamide piperazine compounds) exhibited high apical to basal values (**31**, **32**, **34**, and **35**). The permeability of the compounds was reduced once the side chain amino acid was installed, but metabolic stability is improved (**28** vs **35**). There was no clear correlation between Caco-2 and PAMPA assay. However, the % absorbed was lower in the PAMPA assay for compounds with poor permeability in the Caco-2 assay. Upon comparing the calculated log *P* values with PAMPA as well as Caco-2 values, we discovered no correlation with any of the permeability parameters. Unsurprisingly, log *P* of 4.5 or higher was needed for having excellent percentage absorbed values in PAMPA assay (see Supporting Information). Removing the basicity of the piperazine ring by introduction of carbonyl group improved the mouse and human microsome stability of the compound, presumably by blocking the ethylene bridge (**31** vs **32**) but is

dx.doi.org/10.1021/jm300041e | J. Med. Chem. 2012, 55, 4244−4273

Table 2. SAR Study for Analogues with Substitution on the Piperazine Core

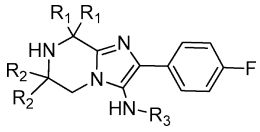

compd	R_1	R_2	R_3	mouse microsome hepatic extraction ratio	*P. falciparum* strain EC_{50} 3D7 (nM)	*P. falciparum* strain EC_{50} W2 (nM)
31	H	H	4-MePh	0.80	161 ± 13	178 ± 12
32	H	=O	4-MePh	0.70	1079 ± 285	1168 ± 188
33	Me	=O	4-MePh	0.72	138 ± 10	136 ± 20
34	Me	=O	3Cl,4F-Ph	0.61	36 ± 2	65 ± 3
35	Me	H	4-MePh	0.77	13 ± 2	13 ± 1
36	Me	H	4-FPh	0.80	5 ± 1	5 ± 1

Table 3. In Vitro ADME of Selected Analogues

entry	PAMPA[a]	Caco-2[b] A–B	Caco-2[b] B–A	CYP Met CL-Ms[c] (ER)	CYP Met CL-rat (ER)	CYP Met CL-Hu[d] (ER)	hERG[e] IC_{50} (μM)
15	52	0.70	2.55	0.47	nt	<0.21	nt
22	51.8	1.26	2.99	0.48	0.66	0.49	13.4
24	51.5	0.61	1.3	0.46	0.69	0.53	>30
27	81	3.05	8.38	0.51	0.63	0.52	5.6
28	99.5	1.2	0.97	0.4	0.89	0.55	21.9
29	99.5	3.5	2.37	0.41	0.79	0.47	>30
31	99.5	8.2	2.36	0.87	0.96	0.79	nt
32	80.9	15	14.37	0.66	0.95	0.44	nt
33	nt	nt	nt	0.72	nt	nt	nt
34	97.1	3.22	3.35	0.61	0.68	0.72	>30
35	99.9	15.56	6.96	0.87	0.93	0.88	nt
36	99.9	nt	nt	0.8	0.92	0.92	nt

[a]Measured as percentage absorbed. [b]units = (cm/s $\times 10^6$). [c]Ms = mouse. [d]Hu = human. [e]Q-patch assay; nt = not tested.

Table 4. Complete in Vivo Pharmacokinetic Profile of Selected Analogues in Mice[a]

	IV PK parameters				PO PK parameters				
entry	V_d (L/kg)	CL (mL/min/kg)	$T_{1/2}$ (h)	$AUC_{(0-24\ h)}$ (h·nM)	C_{max} (nM)	T_{max} (h)	$T_{1/2}$ (h)	$AUC_{(0-24\ h)}$ (h·nM)	F (%)
15	12.3	188.9	2.7	1072	235	2.0	4.20	965	15
22	10.2	49.2	2.0	4119	1538	1.0	4.35	12155	74
24	7.5	27.5	5.5	7062	1723	3.0	5.21	21058	75
27	23.7	60.0	6.2	3442	1803	1.7	8.95	17894	87
29	7.5	36.1	18.0	7607	1642	1.0	14.54	32409	107
34	2.7	12.5	2.8	16525	3651	1.0	2.71	50619	77
36	1.2	25.9	0.8	9090	6404	1.0	2.95	19447	53

[a]PO dosing; dose (mg/kg), 20; species/strain, mouse, male balb/c; formulation, 2.5 mg/mL in PEG300/D5W, 3:1, solution; V_d = volume of distribution; CL = clearance; C_{max} = maximal concentration; T_{max} = time at maximal concentration; AUC = area under the curve; F = oral bioavailability.

not evident in rat microsomes. Introduction of the dimethyl group on the 8-position of the piperazine ring does not improve overall metabolic stability of the compound (**15** vs **28** or **31** vs **35**) despite the metabolite identification results presented earlier. This may be due to the ethylene bridge in the piperazine ring representing a metabolic soft spot and enabling metabolic switching. In general, this scaffold exhibited poor rat metabolic stability when compared to other species. One interesting finding with the substituted piperazine analogues was the improvement of activity against the hERG channel as determined in the automated patch clamp assay. Compared to the unsubstituted piperazine analogue **27**, we were able to decrease inhibition of the hERG channel by at least 2–3-fold, with most analogues (such as **22**) suggesting a lower potential for QT interval prolongation in compounds with a substituted piperazine.

Pharmacokinetic Properties. Compounds series found to have favorable potency and in vitro ADME properties were tested in snapshot PK, an abbreviated PK study shown to accurately bin compounds into low, moderate, or high oral exposure.[9] Compounds predicted to have reasonable oral exposure would be tested in mice using both PO and IV routes of administration (Table 4). The in vivo clearance generally was low to moderate and significantly improved when compared to the corresponding unsubstituted analogues (**15**, **22**). This resulted in higher maximum concentration as well as

dx.doi.org/10.1021/jm300041e | J. Med. Chem. 2012, 55, 4244–4273

improvement in AUC values in the oral arms as well. Lactam compound **34** exhibited highest oral AUC than all other analogues, and it also had lower intrinsic clearance with moderate volume of distribution. To test whether red cell partitioning was occurring to explain the high volume of distribution for the basic compounds, we carried out an in vitro experiment in which compound **22** was incubated in naïve rat whole blood as well as plasma for 30 min. After centrifuging the blood and quantifying the amount of compound in the red blood cells, we determined that the concentration of the compound was 3.47 times higher in whole blood than in plasma alone, indicating that the compound is either adhering to the RBC's or getting distributed inside the cells.

In Vivo Efficacy. Because we had examples of compounds with different modifications with acceptable bioavailability, we decided to carry on the efficacy experiment in mice. The in vivo antimalarial activities of the optimized compounds were evaluated using a *Plasmodium berghei* mouse survival model.[8] In this test, groups of three *P. berghei* infected mice were treated orally with compound one day after infection. The key readouts were the percentage of parasitemia reduction on day 3 postinfection compared to the untreated mice and the prolongation of survival of the infected mice.

Table 5 summarizes the in vivo efficacy test results of compound in comparison with standard antimalarials chloroquine (CQ) and artesunate (AS). It was observed that compounds **22**, **24**, and **29** exhibited >99% parasitemia reduction at a low dose of 30 mg/kg with a modest survival of 15 days or higher. Increasing the dose to 100 mg/kg or dosing the compound 3 × 30 mg/kg did not lead to increase in survival. Currently, we are investigating the possibility of recrudescence of parasites or development of resistance for the compound in vivo to better explain the lack of curative activity in this model. We decided to determine the ED_{99} representative examples for the substituted and nonsubstituted piperazine cores and found the substituted piperazine core was ∼10-fold more efficacious (compound **22** ED_{99} = 2.2 mg/kg) than the unsubstituted core (compound **1** ED_{99} = 26.5 mg/kg). Compounds **34** and **36** clearly proved inferior both in terms of parasitemia reduction as well as survival in mice, indicating the need for the amino acid side chain in providing better mouse efficacy.

Table 5. In Vivo Efficacy of Compounds on *Plasmodium berghei* Mouse Survival Model Following Different Dose Levels in Comparison with Known Antimalarials[a]

	1 × 30 mg/kg		1 × 100 mg/kg		3 × 30 mg/kg	
entry	activity (%)	survival (day)	activity (%)	survival (day)	activity (%)	survival (day)
22	99.5	16.3	99.4	14.0	99.8	17.7
24	99.0	15.0	99.1	16.7	99.7	17.0
29	99.0	15.3	99.0	16.7	99.7	18.0
34	47.0	6.3	97.0	6.7	66.0	7.0
36	90.0	7.0	99.3	9.7	99.7	12.0
CQ[b]	99.5	9.0	99.6	12.5	99.8	13.6
AS[b]	95.6	5.8	98.0	7.0	99.0	12.2

[a]Activity = average parasitemia reduction; survival = average lifespan after infection (6–7 days for untreated control mice); compounds were formulated in 75% PEG300/25% D5W (5% dextrose in water); CQ, chloroquine; AS, artesunate. [b]10% ethanol, 30% PEG400, 6% vitamin ETPGS.

On the basis of the efficacy results, we decided to study the oral exposure of several compounds in rats. Rat was chosen as the second animal species for oral exposure evaluation as it may serve as the in vivo preclinical toxicity species. Taking into account the nonoptimal metabolic stability data for rats for this scaffold, we decided to study the oral exposure of the compound in rat for a period of 5 h in the oral arm only to get an estimation of the exposure (Table 6).[9] The results show that the 8-substituted piperazine compounds had inferior exposure. α-Methylalanine subclass of compounds like **29** did not exhibit any in vivo exposure and were not further pursued. In line with the better rat metabolic stability (ER = 0.68), nonbasic lactam compound **34** demonstrated the best rat exposure despite lower mouse efficacy.

Table 6. Rat Snapshot PK Results for Interesting Compounds[a]

	PK parameters		
entry	$AUC_{(0-5\ h)}$ (h·nM)	C_{max} (nM)	$AUC_{(0-5\ h)}$/dose [(min·μg/mL)/(mg/kg)]
22	487	126	1.2
24	367	96.66	0.95
29	NA	BLQ	
34	2097	504.44	5.07
36	423	202	0.9

[a]PO dosing; dose (mg/kg), 20; species/strain, rat, Wistar; formulation, 2.5 mg/mL in PEG300/D5W, 3:1, solution; BLQ, below level of quantification; NA = could not be determined.

As the oral exposure of compounds **22** was low in rats but demonstrated superior mouse efficacy, we decided to dose compound **22** at higher doses to make sure that sufficient multiples of exposure of the mouse efficacious dose could be achieved (Table 7). We observe that when the dose was increased to 30 mg/kg from 10 mg/kg, there was overproportional 7-fold increase in AUC as well as 2-fold increase in bioavailability. Increasing the dose further to 100 mg/kg dose with suspension formulation led to 55-fold increase in AUC with a 3-fold increase in oral bioavailability. The AUC at the mouse efficacious dose (2 mg/kg) was 780 h·nM, therefore a ∼45× exposure multiple is achieved at 100 mg/kg in the rat. The multiple of exposure provides a sufficient window to use the rat as a rodent toxicology species. It is unclear at this time if this overproportional exposure at higher doses is due to saturating metabolism or an efflux transporter, but given the partial efflux observed in Caco-2, this may explain this multiple dose exposure results.

In Vitro Toxicology. Compound **22** was subjected to a series of assays to evaluate the toxicity profile. This drug candidate was inactive on a panel of human cytochromes P450 (IC_{50s} are greater than 6 μM for CYP1A2, CYP2C19, CYP2C9, CYP2D6, and CYP3A4), and the observed cytotoxicity CC_{50} were all greater than 12 μM on a panel of mammalian cell lines (293T, Ba/F3, CHO, HEp2, HeLa, Huh7), which translates to an adequate selectivity index (SI > 100). Compound **20** was found negative in the mini-Ames and micronucleus tests, which indicated a low mutagenic potential. Finally, considering the efficacious plasma C_{max} in the mouse at 2 mg/kg is low (∼75 nM), the risk of cardiotoxicity is considered to be minimal where the hERG channel inhibitory activity IC_{50} = 13.4 μM, providing a greater than 170-fold window.

dx.doi.org/10.1021/jm300041e | J. Med. Chem. 2012, 55, 4244–4273

Table 7. In Vivo Rat Dose Escalation PK Tests for Compound 22

	IV PK parameters				PO PK parameters					
entry	V_d (L/kg)	CL (mL/min/kg)	$T_{1/2}$ (h)	AUC (h·nM)	dose mg/kg	C_{max} (nM)	T_{max} (h)	$T_{1/2}$ (h)	$AUC_{(all)}$ (h·nM)	F (%)
22	13.7	67.5	4.6	1831	10	91	1.5	4.7	974	20
					30	580	4.3	6.3	7337	40
					100	34885	8.0	8.4	34885	57

SUMMARY

Imidazolopiperazine compounds had been proven to be effective against multidrug resistant parasite strains with minimum toxicity to host-cell lines. However, early lead compound such as compound **15** and **27** still suffer from moderate potencies, relatively poor rat PK, and potent hERG inhibitory activity. Directed by the identification of in vitro metabolites formed by compound **1**, the piperazine core of **15** was systematically modified by a *gem*-dimethyl functionality at all three possible places. The 8,8-dimethyl analogues demonstrated excellent potency as well as improved oral exposure in the mouse. This also allowed us to use the glycine amide that reduced our hERG risk when compared to **27**. The first generation of compounds exhibited efficacy that was comparable to the known antimalarials in the *P. berghei* mouse model, however, compound **22** was more efficacious than chloroquine and artesunate especially when parasitemia reduction is compared in terms of ED_{99} values. Although compound **22** demonstrated poor rat PK at low doses, with higher doses it was able to achieve the necessary exposure multiples calculated based on the plasma concentration found to be efficacious in the mouse model. Compound **22** is thus currently under preclinical safety assessment in rats as a potential candidate for human trials.

EXPERIMENTAL SECTION

Experimental Protocols (Biology). *Maintenance of Plasmodium falciparum Cultures. Plasmodium falciparum* cultures were grown in O^+ RBCs using culturing media: RPMI 1640 media (no phenol red) with L-glutamine and containing 0.05 mg/mL gentamicin, 0.014 mg/mL hypoxanthine, 38.4 mM Hepes, 0.20% sodium bicarbonate, 0.20% glucose, 3.4 nM NaOH, 5% human serum, and 1.25% albumax. Using traditional *P. falciparum* protocols published previously, 25 mL cultures were maintained in 75 cm^2 flasks (Fisher cat. no. 10-126-41) at 5% hematocrit and parasitemia ranging between 1% and 10%.[10] Once parasitemia reached 8−10%, cultures are diluted down to 1% or higher depending on needs. Maintenance required daily media changes and fresh blood every two weeks. Cultures were gassed for approximately 30 s to 1 min using a blood gas mixture to maintain a gas composition of 96% nitrogen, 3% carbon dioxide, and 1% oxygen and incubated at 37 °C. On day 1 of the assay, percent parasitemia was determined by obtaining a 1 μL blood smear. The smear was fixed onto the slide by placing in methanol for 30 s, stained in 10% Geimsa stain, and the percent of parasitized erythrocytes vs uninfected erythrocytes was determined by microscopy with a light microscope.

Antiplasmodial Proliferation Inhibition Assay: 384-Well Plate Format. P. falciparum strains to be used for screening were prepared with screening media (culturing media without human serum but supplemented with 0.5% Albumax II) and fresh erythrocytes. Twenty μL of screening media were dispensed via the MicroFlo (BioTek) into 384-well, black clear-bottom assay plates (μClear GNF custom plates by Griener Bio-One). Then 50 nL of compounds were transferred using a PlateMate Plus (Matrix) or the GNF Systems PinTool into the assay plates containing screening media to a final maximum concentration of 10 μM in a 12 point dose−response (1/2 log serial dilution). On the basis of the measured parasitemia levels, each parasite strain was diluted to yield 0.5% parasitemia, and 50% hematocrit blood (uninfected erythrocytes) was added to a concentration of 4.17%. This diluted culture was used in dispensing the remaining 60% of the assay volume (30 μL) into the prewarmed assay plates via the MicroFlo liquid dispenser. The final parasitemia was 0.3% and final hematocrit was 2.5% in a total volume of 50 μL. Assay plates were incubated at 37 °C for 72 h in a gas chamber filled with low oxygen blood gas. After the 72 h incubation (equivalent to 1−2 cycles during the blood stage), a prepared mixture of the lysis buffer (5 mM EDTA, 1.6% Triton X-100, 20 mM Tris-HCl, 0.16% saponin) in water and SYBR Green detection (0.1%) reagent was dispensed at 10 μL per well using the MicroFlo. Cultures were incubated for an additional 24 h at 25 °C before measuring fluorescence intensity using the Envision plate reader (Perkin-Elmer) with a 505 dichroic mirror. Excitation and emission filters are 485 and 530 nm, respectively. Data were normalized based on maximum fluorescence signal values for DMSO treated wells (no inhibition by compound) and the minimum fluorescence signal values for wells containing the highest concentration of inhibitor control compounds, for example, pyrimethamine at a final concentration of 10 μM. Data were analyzed on a plate-by-plate basis and compared to reference compounds that were always included on every plate, typically artemisinin, mefloquine, and pyrimethamine. EC_{50} values were obtained using a custom curve fitting model, and a standard logistic regression model was applied for curve fitting. The quality of the assay run was assessed by the performance of the reference compounds where the EC_{50} must be within 3-fold of the standard reference values for the assay plate to pass requisite data quality control needs. Additionally, all compounds were typically assayed at a minimum in duplicate (independent assay plates) and EC_{50} values ideally must not vary by more than 2-fold between plates.

Metabolic Stability. The metabolic stability of drug candidates was determined in human, mouse, and rat liver microsomes using the compound depletion approach, quantified by LC/MS/MS. The assay measured the rate and extent of metabolism of chemical compounds by measuring the disappearance of the parent compound. The assay determined the compound's in vitro half-life ($T_{1/2}$) and hepatic extraction ratios (ER) and predicted metabolic clearance in human, rat, and mouse species.[11]

PAMPA Assay. Permeation experiments were carried out in 96-well microtiter filter plates. The compound concentration was determined by UV absorption measured with a SpectraMax190 microplate spectrophotometer (Molecular Devices Corporation, Sunnyvale, CA, USA) at absorption wavelengths between 260 and 290 nm.[12]

Caco-2 Assay. The Caco-2 assay was carried out in a 96-well format, and compound concentrations in each chamber were measured by LC/MS. The assay offers apparent permeability data of test compounds from the apical to the basolateral chambers [P_{app} (A−B)] and from the basolateral to the apical chambers [P_{app} (B−A)]. The results can be used to predict the in vivo oral absorption (using P_{app} (A−B)) and the transport mechanism of the test compounds across GI membrane (ratio of P_{app} (B−A):P_{app} (A−B) and log P lipophilicity data).[13]

hERG (Q-Patch) Assay. The assay utilizes electrophysiology measurement on the electric current passing through hERG channel that is heterologously expressed in a stable CHO cell line. Channels were open by a hERG-specific voltage protocol, and the compound effects were directly characterized by their block of the hERG current. The assay was performed on an automated platform, Q-Patch. All

dx.doi.org/10.1021/jm300041e | J. Med. Chem. 2012, 55, 4244−4273

compounds were tested by 4-point dose−response curves, and IC_{50} values (between 0.2 and 30 μM) were measured.[14]

In Vivo PK. *In Vivo Pharmacokinetics Studies in Mice.* In-life studies were carried out under protocols approved by the Animal Care and Use Committee (IACUC) of GNF. All compounds were formulated at a concentration of 2.5 mg/mL in 75% PEG300 and 25% D5W (5% dextrose in distilled water) solution and were filtered using a 0.45 μm syringe filter. The filtered solutions were dosed intravenously via the lateral tail vein at 5 mg/kg with a dosing volume of 2 mL/kg to male Balb/c mice (n = 3 per group). The filtered solutions were also administered orally at 20 mg/kg (with a dosing volume of 8 mL/kg) to another group of mice (n = 3 per group). Six blood samples of 50 μL each were collected serially from each animal via retro orbital sinus up to 24 h after dosing. Blood samples were collected into heparin microtainer and centrifuged and plasma separated and frozen until analysis. Plasma samples were analyzed by LC-MS/MS.

In Vivo Pharmacokinetics Studies in Rats (Snapshot and Full PK). Compounds were formulated at a concentration of 2.5 mg/mL in 75% PEG300 and 25% D5W solution. In rat snapshot PK, two rats (Wistar rats) were administrated orally at 10 mg/kg dose and four blood samples (100 μL) were taken at 0.5, 1, 3, and 5 h post dosing. Before the sample analysis, the plasma samples were pooled based on the sampling time. In the rat full PK studies, the formulations were filtered before the administration to rats. Three rats were dosed intravenously (3 mg/kg), and three rats were administrated orally (10 mg/kg). Six blood samples (100 μL per sample) were collected serially from each rat within 24 h post dosing.

Extraction and LCMS Analysis. Plasma samples (20 μL) were extracted with solution of acetonitrile:methanol (3:1) containing internal standard. The samples were vortexed and then centrifuged with an Eppendorf centrifuge 5810R (Eppendorf, Hamburg, Germany) at a setting of 4000 rpm for 5 min at 4 °C. The supernatant was transferred to a clean 96-well analysis plate for LC/MS/MS analysis. An aliquot (10 μL) was injected onto a Phenomenex C18 guard column (4 mm × 2 mm) followed by a Zorbax SB-C8 analytical column (2.1 mm × 30 mm, 3.5 μm, Agilent Technologies Inc., Palo Alto, CA, USA). Separation was carried out using a gradient elution method with a mobile phase consisting of 0.05% formic acid in water (solvent A) and 0.05% formic acid in acetonitrile (solvent B). The flow rate was 600 μL/min. The HPLC system, consisting of Agilent 1100 series binary pump (Agilent Technologies Inc.), Agilent 1100 series micro vacuum degasser (Agilent Technologies Inc.), HTC PAL CTC analytics autosampler (LEAP Technologies, Carborro, NC), and VICI two-position actuator (Valco Int., Houston, TX, USA) was interfaced to a MDS SCIEX API-4000 triple quadruple mass spectrometer (MDS Inc., Toronto, Canada). Mass spectral analyses were carried out using electrospray source in the positive ion mode and using multiple reaction monitoring (MRM) for quantification. MRM transition of compound **15** 383.9/101.2, compound **22** 412.2/312.1, compound **24** 430.1/330.1, compound **27** 412.2/327.2, compound **29** 436.1/308.1, compound **34** 430.0/346.1, and compound **36** 355.0/272.3 was used with its optimized MS parameters, respectively.

Pharmacokinetic Analysis. The mean value from the three animals at each time point was plotted against time to give plasma concentration time profile. Pharmacokinetic parameters were determined using Watson LIMS, version 7.2 (Thermo Electron Corporation, PA, USA), by noncompartmental analysis. Pharmacokinetic parameters for compounds were calculated by noncompartmental regression analysis using an in-house fitting program developed at GNF. The oral bioavailability (F) was calculated as the ratio between the area under the curve (AUC) following oral administration and the AUC following intravenous administration corrected for dose (F = $AUC_{po} \times dose_{iv}/AUC_{iv} \times dose_{po}$).

In Vivo Antimalarial Activity. All in vivo efficacy studies were approved by the veterinary authorities of the Canton Basel-Stadt. In vivo antimalarial activity was usually assessed for groups of three female NMRI mice (20−22 g) intravenously infected on day zero with 2×10^7 erythrocytes parasitized with *P. berghei* GFP ANKA malaria strain (PbGFPCON donation from A. P. Waters and C. J. Janse, Leiden University).[8a,15] Untreated control mice die typically between day six and day seven post infection. Experimental compounds were formulated in 75% PEG300/25% D5W as indicated. Chloroquine and artesunate were formulated in 10% ethanol, 30% PEG400, and 6% vitamin E TPGS. Compounds were administered orally in a volume of 10 mL/kg either as a single dose (24 h post infection) or as three consecutive daily doses (24, 48, and 72 h post infection). With the single dose regimen, parasitemia was determined (72 h post infection) and for the triple dose regimen (96 h post infection) using standard flow cytometry techniques.[15] Activity was calculated as the difference between the mean percent parasitemia for the control and treated groups expressed as a percentage of the control group. The survival time in days was also recorded up to 30 days after infection. A compound was considered curative if the animal survived to day 30 after infection with no detectable parasites.

Experimental Protocols (Chemistry). *Materials and Methods.* Unless otherwise noted, materials were obtained from commercial suppliers and were used without purification. Removal of solvent under reduced pressure refers to distillation using Büchi rotary evaporator attached to a vacuum pump (∼3 mmHg). Products obtained as solids or high boiling oils were dried under vacuum (∼1 mmHg). Purification of compounds by high pressure liquid chromatography was achieved using a Waters 2487 series with Ultra 120 5 μm C18Q column with a linear gradient from 10% solvent A (acetonitrile with 0.035% trifluoroacetic acid) in solvent B (water with 0.05% trifluoroacetic acid) to 90% A in 7.5 min, followed by 2.5 min elution with 90% A.

^{1}H NMR spectra were recorded on Bruker XWIN-NMR (400 or 600 MHz). Proton resonances are reported in parts per million (ppm) downfield from tetramethylsilane (TMS). ^{1}H NMR data are reported as multiplicity (s singlet, d doublet, t triplet, q quartet, quint quinted, sept septed, dd doublet of doublets, dt doublet of triplet, bs broad singlet), number of protons, and coupling constant in hertz. For spectra obtained in $CDCl_3$, DMSO-d_6, and CD_3OD, the residual protons (7.27, 2.50, and 3.31 ppm, respectively) were used as the reference.

Analytical thin-layer chromatography (TLC) was performed on commercial silica plates (Merck 60-F 254, 0.25 mm thickness); compounds were visualized by UV light (254 nm). Flash chromatography was performed either by CombiFlash (separation system Sg. 100c, ISCO) or using silica gel (Merck Kieselgel 60, 230−400 mesh). The purity and quantitative analysis were determined with a Waters ZQ 2000 LC/MS system, which employed an Acquity UPLC system (binary pump, column compartment, autosampler, and diode array UV detector). The eluent was split between the mass spectrometer and an Antek chemiluminescent nitrogen detector (CLND). The mobile phases used were (A) 95% H_2O/5% MeOH/IPA (75/25, v/v) + 0.05% formic acid and (B) MeOH/IPA (75/25, v/v) + 0.035% formic acid. A gradient HPLC method with flow of 0.4 mL/min started at 2% B, with a hold of 1.0 min before a linear increase to 95% B at 3.50 min, with a 30 s hold. From 4.0−4.25 min, the mobile phases were returned to starting conditions. Total run time was 5.0 min. The column used was a Thermo Syncronis C18 2.1 mm × 30 mm, 3 μm. The mass spectrometer was operated in positive mode, with a spray voltage of 3.2 kV and cone voltage of 30 V. The source and desolvation temperatures were 130 and 400 °C, respectively, with 600 L/h of nitrogen desolvation flow. All the final compounds reported in this communication had the purity of at least 95%. Elemental analyses were carried out by Midwest microlabs LLC, Indianapolis, IN, USA.

Synthesis of 1a. Compound **1a** was prepared from **1** by the following method: to a stirred solution of **1** (12 mg, 0.03 mmol) was added MnO_2 (52 mg, 0.60 mmol). The reaction mixture was stirred at room temperature (rt) for 2 h. LC/MS test showed that **1** was almost consumed and the desired product ([M + 1] = 428) was detected as one of the major peaks. Solid was filtered off, and solvent was

removed. The residue was subjected to a mass-triggered HPLC purification to give **1a** as well as **1b**.

^{1}H NMR for **1a** (400 MHz, CD_3OD) δ 7.59−7.63 (m, 2H), 7.09 (t, J = 6.4 Hz, 2H), 6.95−7.02 (m, 1H), 6.46−6.52 (m, 1H), 6.34−6.38 (m, 1H), 5.92 (s, 1H), 4.33 (dd, J = 4.4, 14 Hz, 1H), 3.96 (dd, J = 4.8, 13.2 Hz, 1H), 3.70−3.78 (m, 1H), 3.46−3.54 (m, 1H), 1.73 (s, 3H), 1.36 (s, 3H). m/z = 428.1 (M + 1). ^{1}H NMR for **1b** (400 MHz, CD_3OD) δ 7.75−7.78 (m, 2H), 6.95−7.01 (m, 3H), 6.44−6.50 (m, 1H), 6.32−6.36 (m, 1H), 4.19 (dd, J = 1.6, 6.8 Hz, 2H), 4.00 (dd, J = 1.6, 6.8 Hz, 2H), 1.47 (s, 6H). m/z = 426.1 (M + 1).

Synthesis of ***10*** *(R_1=R_2=Me).* To a solution of 2-bromo-1-(4-fluorophenyl)ethanone (46.5 g, 214.29 mmol) in DMF (400 mL) was

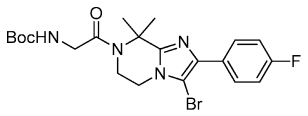

10

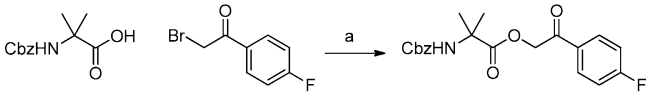

2 **3** **4**

added 2-(benzyloxycarbonyl)-2-methylpropanoic acid (55.8 g, 236.4 mmol) and potassium carbonate (35.4 g, 256.5 mmol). The resulting solution was stirred for 4 h at rt. The resulting solution was diluted with 1000 mL of water. The resulting solution was extracted with ethyl acetate (2 × 800 mL), and the combined organic layer was washed with water (2 × 800 mL) and then brine (1 × 800 mL). The resulting

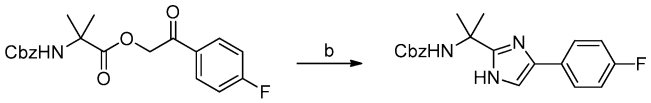

4 **5**

organic phase was concentrated under vacuum. This resulted in 67 g (84%) of compound **4** as a white solid. m/z = 374 (M + 1).

To a solution of compound **4** (70 g, 187.7 mmol) in toluene (700 mL) was added NH_4OAc (144.5 g, 1.88 mol). The resulting solution was heated to reflux for 3 h in an oil bath. The resulting mixture was concentrated under vacuum. The residue was dissolved in 800 mL of water. The resulting solution was extracted with ethyl acetate (2 × 500 mL), and the combined organic layer was washed with water (2 × 800 mL) and brine (1 × 800 mL). The resulting mixture was concentrated under vacuum. This resulted in 58 g (88%) of compound **5** as a white solid. ^{1}H NMR

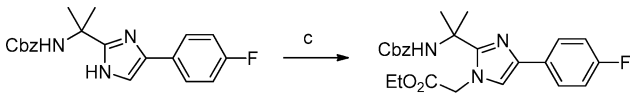

5 **6**

(300 Hz, DMSO-d_6) δ 11.91 (s, NH), 7.80−7.75 (m, 2H), 7.54−7.12 (m, 8H), 4.97 (m, 2H), 1.6 (s, 6H).

To a solution of compound **5** (58 g, 164.3 mmol) in DMF (400 mL) was added cesium carbonate (134 g, 411.0 mmol). This was followed by the addition of ethyl 2-bromoacetate (33 g, 197.6 mmol) dropwise with stirring at rt in 30 min. The resulting solution was stirred for 2 h at rt. The resulting solution was diluted with 1000 mL of water/ice. The resulting solution was extracted with ethyl acetate (2 × 700 mL), and the combined organic layer was washed with water (2 × 800 mL) and brine (1 × 800 mL). The resulting mixture was dried concentrated under vacuum. This resulted in 60 g (83%) of compound **6** as a yellow solid. ^{1}H NMR (300 Hz, DMSO-d_6) δ 7.76−7.72 (m, 2H), 7.32−7.28 (m, 5H), 7.08−7.03 (m, 3H), 5.08 (m, 2H), 4.87 (m, 2H), 4.23 (q, J = 5.4 Hz, 2H), 2.0 (s, 6H), 1.28 (t, J = 5.4 Hz, 3H).

To a solution of compound **6** (70 g, 159.45 mmol, 1.00 equiv) in methanol (800 mL) was added palladium on carbon (10 g). The resulting solution was degassed and backfilled with hydrogen. The solution was stirred for 3 days at 25 °C. The solids were filtered out

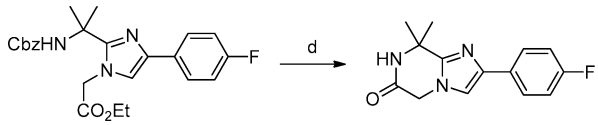

6 **7**

and washed with MeOH. The filtrate was concentrated under reduced pressure. This resulted in **7** (38 g, 145.56 mmol, 91%) as a white solid. LC-MS: (ES, m/z) $[M + H]^+$ calcd for $C_{14}H_{14}FN_3O$, 260; found, 260.

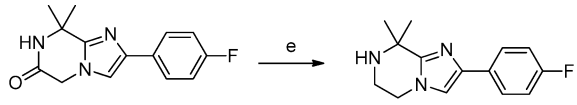

7 **8**

^{1}H NMR (300 Hz, DMSO-d_6) δ 7.79−7.74 (m, 2H), 7.13−7.07 (m, 3H), 6.35 (s, 1H), 4.73 (s, 2H), 1.79 (s, 6H).

To a stirred solution of compound **7** (5 g, 19.2 mmol, 1 equiv) was dissolved in 50 mL of THF, 1 M borane/THF complex (57 mL, 57 mmol, 3 equiv) was added slowly and reaction was refluxed overnight. LCMS indicated that the reaction was complete. THF was removed under reduced pressure. The reaction was quenched with MeOH. The crude product of **8** (4.5 g, 18.3 mmol, 95%) was used in the next step. LC-MS: (ES, m/z) $[M + H]^+$ calcd for $C_{14}H_{17}FN_3$ 246, found 246. ^{1}H NMR (DMSO, 300 Hz) δ 7.75−7.70 (m, 2H), 7.4 (s, 1H), 7.14 (t, J =

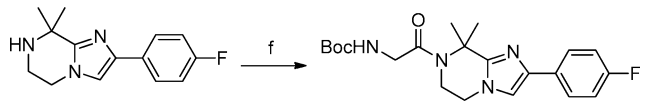

8 **9**

9.0 Hz, 2H), 3.9 (t, J = 5.4 Hz, 2H), 2.51 (t, J = 5.4 Hz, 2H), 1.41(s, 6H); NH proton not observed.

To a stirred solution of compound **8** (2.9 g, 11.82 mmol, 1.1 equiv) and 2-(*tert*-butoxycarbonylamino)acetic acid (2.27 g, 13 mmol, 1.1 equiv) in 15 mL of dichloromethane were added DIEA (2.47 mL, 14.18 mmol, 1.2 equiv) and HATU (5.39 g, 14.18 mmol, 1.2 equiv). The reaction mixture was stirred at rt for 8 h. HPLC/MS analysis showed that desired product compound **9** was the major product. The reaction was further diluted with dichloromethane (70 mL). The organic layer was washed with washed with water (1 × 30 mL), followed by saturated $NaHCO_3$ (1 × 30 mL) and finally with brine (1 × 30 mL). The organic layer was then dried over anhydrous Na_2SO_4 and concentrated in vacuo. The resulting oil was purified using column chromatography with hexanes/ethyl acetate (0−100% linear gradient) used as eluant. The desired product compound **9** was obtained as oil (3.3 g, 8.27 mmol, 70%). ^{1}H NMR (300 Hz, DMSO-d_6,) δ 7.77−7.72 (m, 2H), 7.54 (s, 1H), 7.20−7.14 (m, 2H), 6.84−6.80 (m, 1H), 4.07 (s, 2H), 3.90 (d, J = 3.0 Hz, 2H), 3.70 (s, 2H), 1.80 (s, 6H), 1.40 (s,

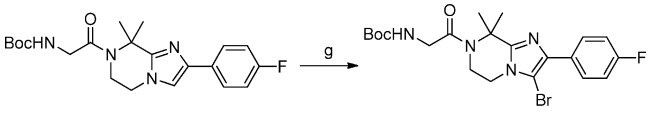

9 **10**

9H). LC-MS: (ES, m/z) $[M + H]^+$ calcd for $C_{21}H_{28}FN_4O_3$, 403; found, 403.

To a stirred solution of compound **9** (3.02 g, 7.51 mmol) in dichloromethane (30 mL) was added Br_2 (0.43 mL, 8.26 mmol) in acetic acid (3 mL). The reaction mixture was stirred at rt for 30 min.

dx.doi.org/10.1021/jm300041e | J. Med. Chem. 2012, 55, 4244−4273

HPLC/MS test showed that desired product (II) was the only peak. Solvent was removed via rotavap at a temperature no higher than 20 °C. After neutralization, white solid (3.60 g) was obtained. The product was confirmed by 400 MHz proton NMR to be the title compound **10**. The product was used in the next step without further purification and exhibited quantitative mass recovery. LC-MS: (ES, m/z) $[M + H]^+$ calcd for $C_{21}H_{27}BrFN_4O_3$, 482; found, 482. ^{1}H NMR (MeOH-d_4, 400 Hz) δ 7.84−7.81 (m, 2H), 7.14 (t, J = 8.8 Hz, 2H), 4.09−4.01 (m, 4H), 3.81 (t, J = 4.8 Hz, 2H), 1.89 (s, 6H), 1.46 (s, 9H).

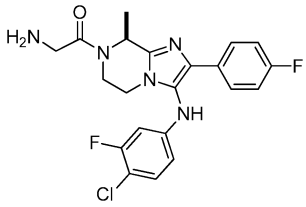

Synthesis of ***17****.* (*S*)-2-Amino-1-(3-(4-chloro-3-fluorophenylamino)-2-(4-fluorophenyl)-8-methyl-5,6-dihydroimidazo[1,2-*a*]pyrazin-7(8*H*)-yl)ethanone:

Compound **17** was prepared from compound **10** (R_1 = Me, R_2 = H) by a $Pd_2(dba)_3$ mediated amination reaction with 4-chloro-3-fluoroaniline followed by a TFA mediated deprotection in a protocol similar to compound **22**. ^{1}H NMR (MeOH-d_4, 400 MHz) δ 7.61−7.58 (m, 2H), 7.16−7.12 (m, 1H), 7.07−7.02 (m, 2H), 6.47−6.42 (m, 2H), 5.74 (m, 1H), 4.07−3.68 (m, 6H), 1.56 (d, J = 6.8 Hz, 3H). m/z = 432.0 (M + 1).

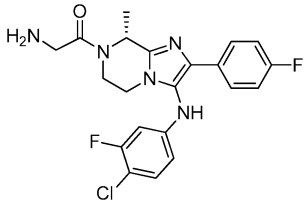

Synthesis of ***18****.* (*R*)-2-Amino-1-(3-(4-chloro-3-fluorophenylamino)-2-(4-fluorophenyl)-8-methyl-5,6-dihydroimidazo[1,2-*a*]pyrazin-7(8*H*)-yl)ethanone:

Compound **18** was prepared from compound **10** (R_1 = Me, R_2 = H) by a $Pd_2(dba)_3$ mediated amination reaction with 4-chloro-3-fluoroaniline followed by a TFA mediated deprotection in a protocol similar to compound **22**. m/z = 432.2 (M + 1).

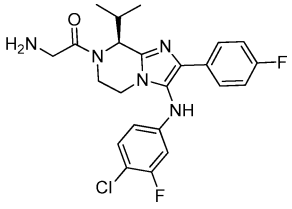

Synthesis of ***19****.* (*S*)-2-Amino-1-(3-(4-chloro-3-fluorophenylamino)-2-(4-fluorophenyl)-8-isopropyl-5,6-dihydroimidazo[1,2-*a*]pyrazin-7(8*H*)-yl)ethanone:

Compound **19** was prepared from compound **10** (R_1 = isopropyl, R_2 = H) by a $Pd_2(dba)_3$ mediated amination reaction with 4-chloro-3-fluoroaniline followed by a TFA mediated deprotection in a protocol similar to compound **22**. ^{1}H NMR (MeOH-d_4, 400 MHz) δ7.61−7.58 (m, 2H), 7.26−7.20 (m, 3H), 6.45−6.38 (m, 2H), 5.5 (d, J = 7.9 Hz, 1H), 4.11−3.75 (m, 6H), 2.36−2.31 (m, 1H), 1.15 (d, J = 6.7 Hz, 3H), 0.95 (d, J = 6.7 Hz, 3H). m/z = 460.2 (M + 1).

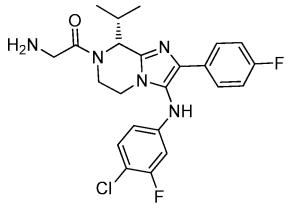

Synthesis of ***20****.* (*R*)-2-Amino-1-(3-(4-chloro-3-fluorophenylamino)-2-(4-fluorophenyl)-8-isopropyl-5,6-dihydroimidazo[1,2-*a*]pyrazin-7(8*H*)-yl)ethanone:

Compound **20** was prepared from compound **10** (R_1 = isopropyl, R_2 = H) by a $Pd_2(dba)_3$ mediated amination reaction with 4-chloro-3-fluoroaniline followed by a TFA mediated deprotection in a protocol similar to compound **22**. ^{1}H NMR (MeOH-d_4, 400 MHz) δ 7.69−7.67 (m, 2H), 7.27−7.20 (m, 3H), 6.68−6.65 (dd, J = 2.5 Hz, J = 11.0 Hz, 1H), 6.60−6.55 (dd, J = 2.25 Hz, J = 8.7 Hz, 1H), 5.78 (d, J = 7.7 Hz, 1H), 4.42−4.02 (m, 4H), 3.94−3.87 (m, 2H), 2.55 (m,1H), 1.24(d, J = 6.8 Hz, 3H), 1.05 (d, J = 6.8 Hz, 3H). m/z = 460.2 (M + 1).

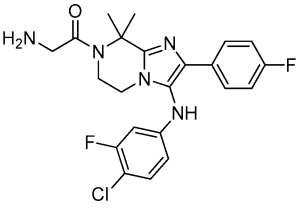

Synthesis of ***21****.* 2-Amino-1-(3-(4-chloro-3-fluorophenylamino)-2-(4-fluorophenyl)-8,8-dimethyl-5,6-dihydroimidazo[1,2-*a*]pyrazin-7(8*H*)-yl)ethanone:

Compound **21** was prepared from compound **10** (R_1 = Me, R_2 = Me) by a $Pd_2(dba)_3$ mediated amination reaction with 4-chloro-3-fluoroaniline followed by a TFA mediated deprotection in a protocol similar to compound **22**.

^{1}H NMR (MeOH-d_4, 400 MHz) δ 7.59−7.55 (m, 2H), 7.20−7.13 (m, 3H), 6.60 (dd, J = 11.2, 10.8 Hz), 1H), 6.53 (dd, J = 2.4, 0.8 Hz, 1H), 4.0 (m, 4H), 3.78 (m, 2H), 2.00 (s, 6H). m/z = 446.0 (M + 1). Elemental analysis (compound + 2.0 HCl + 2.0 H_2O): % C, 47.62; % H, 5.09; %N, 12.62; (calc). %C = 47.54/47.38; %N = 12.44/12.46; % H = 4.62/4.57 (experimental). LC/MS major mass 446.2.

Synthesis of ***22*** *(Analogue of Compound* ***12*** *in Scheme 2 where* R_1=R_2=*Me).* 2-Amino-1-(2-(4-fluorophenyl)-3-(4-fluorophenylamino)-8,8-dimethyl-5,6-dihydroimidazo[1,2-*a*]pyrazin-7(8*H*)-yl)ethanone:

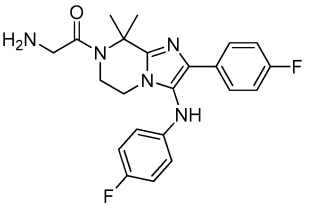

In a glass vial, Cs_2CO_3, 4F-aniline (0.462 g, 4.1 mmol, 2.0 equiv), $Pd_2(dba)_3$ (0.095 g, 0.104 mmol, 0.05 equiv), xantphos (0.120 g, 0.208 mmol, 0.1 equiv), and dioxane were stirred for 5 min at rt. Compound **10** (1 g, 2.08 mmol, 1.0 equiv) was added to the reaction mixture, after which the reaction mixture was degassed for 15 min and then stirred at 120 °C under N_2 for 8 h. HPLC/MS test showed that the starting material compound **10** was consumed and desired product was formed predominantly along with some **9**. The reaction was filtered to remove solids. The reaction mixture was concentrated and then purified by normal phase column chromatography (silica gel 80 g) using a gradient of 100−0% to 0−100% hexane:EtOAc. The desired product eluted at 60:40 EtOAc:hexanes. The organic layer was concentrated at reduced pressure to yield the Boc derivative (950 mg, 89%) yield.

dx.doi.org/10.1021/jm300041e | *J. Med. Chem.* 2012, 55, 4244−4273

Table 8. Regiochemistry of the diMe Groups Assigned Using 2-D NMR Techniques

^{1}H NMR (400 MHz, DMSO-d_6) δ ppm 1.85 (s, 16 H) 3.37 - 3.43 (m, 4 H) 3.63 (d, *J*=5.12 Hz, 5 H) 3.68 (d, *J*=5.12 Hz, 5 H) 6.52 - 6.58 (m, 5 H) 6.99 (t, *J*=8.88 Hz, 5 H) 7.14 (t, *J*=8.96 Hz, 5 H) 7.79 (dd, *J*=8.96, 5.72 Hz, 5 H) 7.83 (s, 2 H)

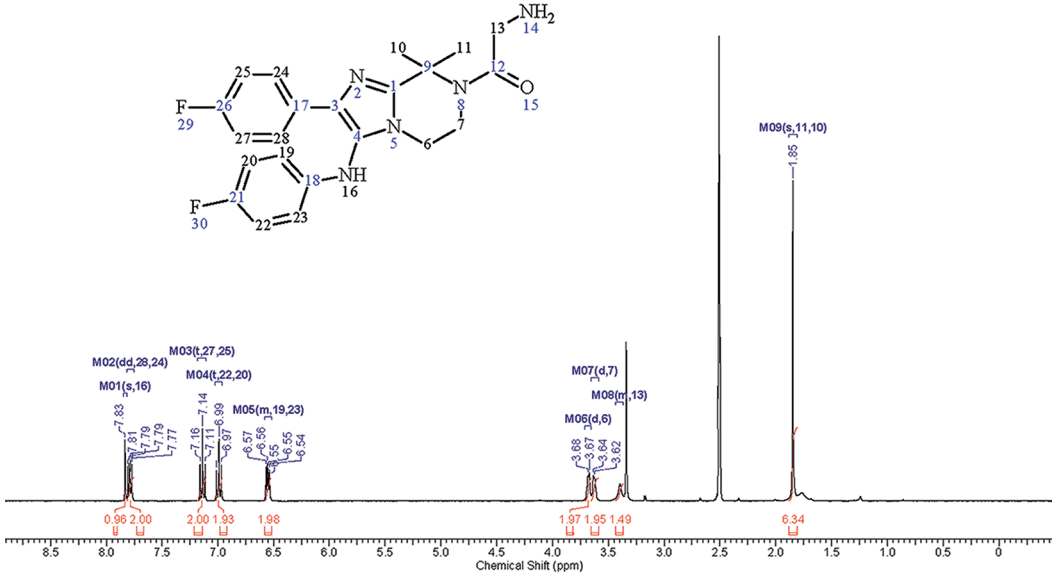

No.	Atom	Exp. Shift (ppm)	Multiplet	No.	Atom	Exp. Shift (ppm)	Multiplet
1	6	3.68	M06	8	20	6.99	M04
2	7	3.63	M07	9	22	6.99	M04
3	10	1.85	M09	10	23	6.55	M05
4	11	1.85	M09	11	24	7.79	M02
5	13	3.4	M08	12	25	7.14	M03
6	16	7.83	M01	13	27	7.14	M03
7	19	6.55	M05	14	28	7.79	M02

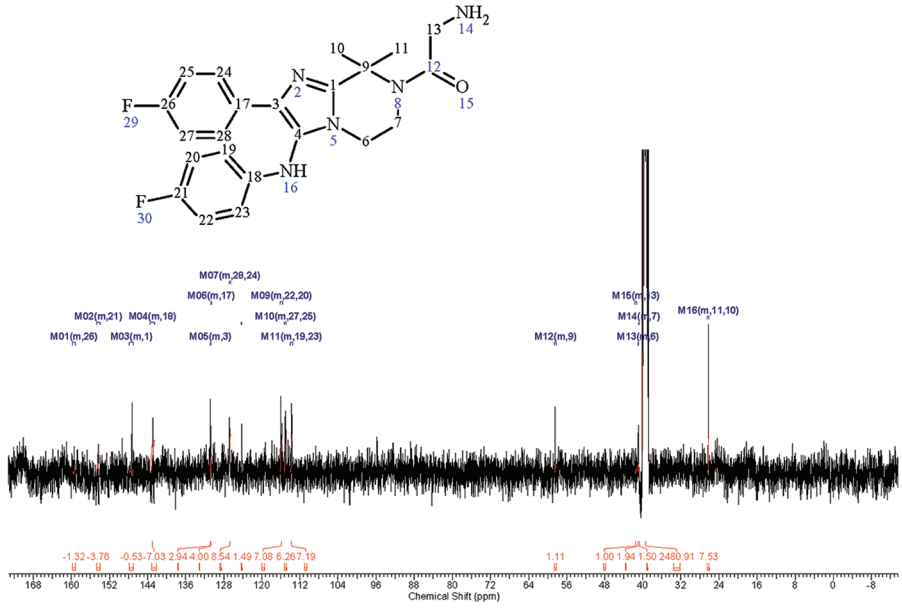

No.	Atom	Exp. Shift (ppm)	Multiplet	No.	Atom	Exp. Shift (ppm)	Multiplet
1	1	147.43	M03	3	4	124.26	M08
2	3	130.8	M05	4	6	40.99	M13

dx.doi.org/10.1021/jm300041e | *J. Med. Chem.* 2012, 55, 4244−4273

Table 8. continued

No.	Atom	Shift (ppm)	Multiplet	No.	Atom	Shift (ppm)	Multiplet
5	7	40.83	M14	14	21	154.35	M02
6	9	58.4	M12	15	22	115.9	M09
7	10	26.24	M16	16	23	113.76	M11
8	11	26.24	M16	17	24	126.71	M07
9	13	41.48	M15	18	25	115.04	M10
10	17	130.64	M06	19	26	159.44	M01
11	18	143.03	M04	20	27	115.04	M10
12	19	113.76	M11	21	28	126.71	M07
13	20	115.9	M09				

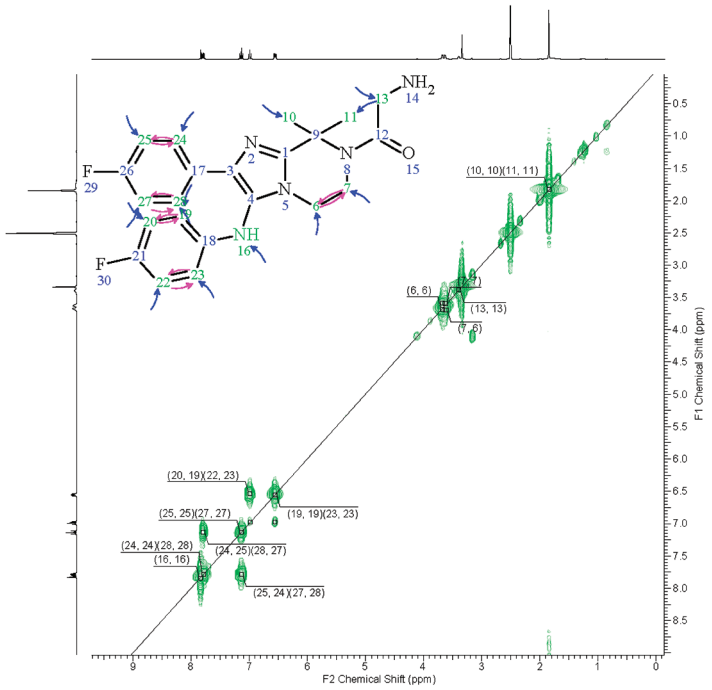

No.	F2 Atom	F1 Atom	F2 (ppm)	F1 (ppm)	No.	F2 Atom	F1 Atom	F2 (ppm)	F1 (ppm)
1	6	6	3.67	3.68	13	22	22	6.98	6.98
2	7	6	3.62	3.69	14	23	22	6.55	6.98
3	6	7	3.68	3.59	15	22	23	6.99	6.54
4	7	7	3.62	3.59	16	23	23	6.55	6.56
5	10	10	1.84	1.82	17	24	24	7.78	7.78
6	11	11	1.84	1.82	18	25	24	7.14	7.78
7	13	13	3.39	3.38	19	24	25	7.79	7.13
8	16	16	7.83	7.84	20	25	25	7.14	7.13
9	19	19	6.55	6.56	21	27	27	7.14	7.13
10	20	19	6.99	6.54	22	28	27	7.79	7.13
11	19	20	6.55	6.98	23	27	28	7.14	7.78
12	20	20	6.98	6.98	24	28	28	7.78	7.78
13	22	22	6.98	6.98					

dx.doi.org/10.1021/jm300041e | J. Med. Chem. 2012, 55, 4244−4273

Table 8. continued

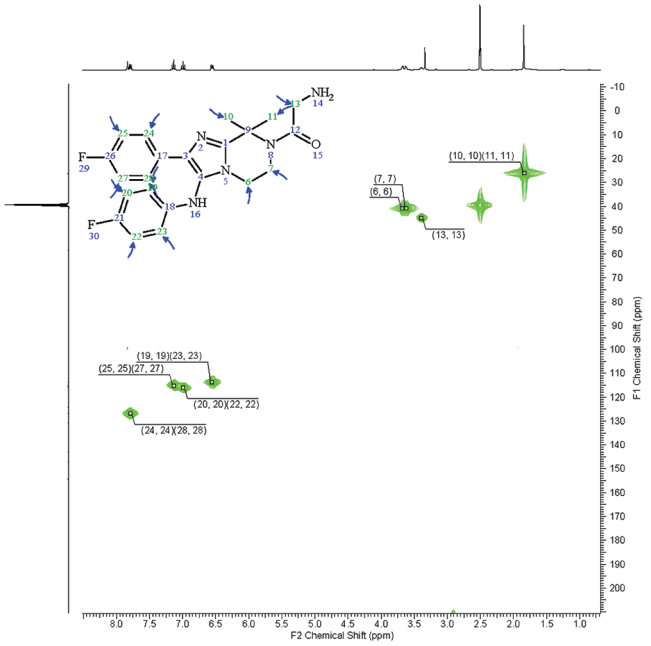

No.	F2 Atom	F1 Atom	F2 (ppm)	F1 (ppm)	No.	F2 Atom	F1 Atom	F2 (ppm)	F1 (ppm)
1	6	6	3.68	40.89	8	22	22	6.99	115.94
2	7	7	3.62	40.92	9	23	23	6.55	113.69
3	10	10	1.84	26.04	10	24	24	7.79	126.84
4	11	11	1.84	26.04	11	25	25	7.13	115.12
5	13	13	3.39	44.88	12	27	27	7.13	115.12
6	19	19	6.55	113.69	13	28	28	7.79	126.84
7	20	20	6.99	115.94					

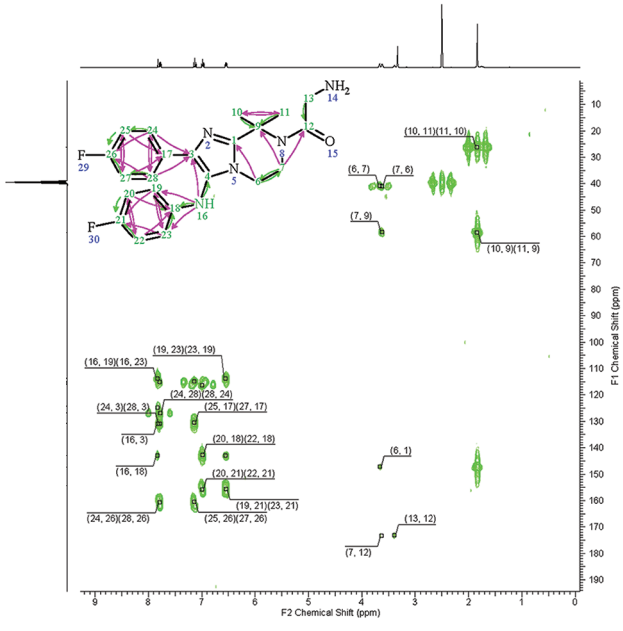

No.	F2 Atom	F1 Atom	F2 (ppm)	F1 (ppm)	No.	F2 Atom	F1 Atom	F2 (ppm)	F1 (ppm)
1	6	1	3.66	147.14	3	24	3	7.79	130.83
2	16	3	7.82	130.82	4	28	3	7.79	130.83

dx.doi.org/10.1021/jm300041e | J. Med. Chem. 2012, 55, 4244−4273

Table 8. continued

No.	F2 Atom	F1 Atom	F2 (ppm)	F1 (ppm)	No.	F2 Atom	F1 Atom	F2 (ppm)	F1 (ppm)
5	16	4	7.83	124.77	24	22	20	6.99	116.22
6	7	6	3.62	40.96	25	19	21	6.55	155.68
7	6	7	3.67	40.7	26	20	21	6.99	155.86
8	7	9	3.62	58.38	27	22	21	6.99	155.86
9	10	9	1.84	58.5	28	23	21	6.55	155.68
10	11	9	1.84	58.5	29	20	22	6.99	116.22
11	11	10	1.84	26.29	30	16	23	7.83	113.74
12	10	11	1.84	26.29	31	19	23	6.56	113.75
13	7	12	3.63	173.36	32	28	24	7.78	126.82
14	13	12	3.39	173.07	33	24	25	7.79	114.99
15	25	17	7.14	130.47	34	27	25	7.14	114.94
16	27	17	7.14	130.47	35	24	26	7.79	160.61
17	16	18	7.83	142.87	36	25	26	7.14	160.51
18	19	18	6.55	143.02	37	27	26	7.14	160.51
19	20	18	6.99	142.8	38	28	26	7.79	160.61
20	22	18	6.99	142.8	39	25	27	7.14	114.94
21	23	18	6.55	143.02	40	28	27	7.79	114.99
22	16	19	7.83	113.74	41	24	28	7.78	126.82
23	23	19	6.56	113.75					

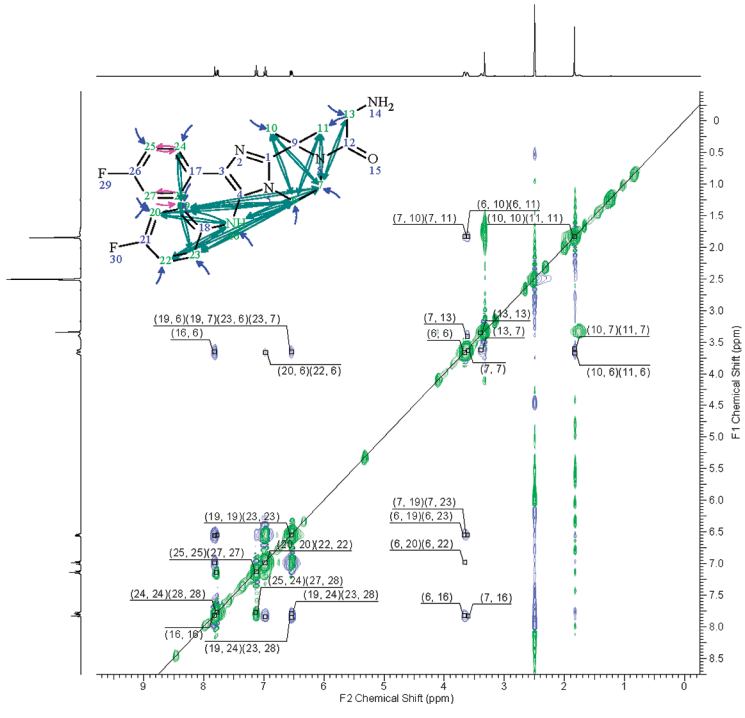

No.	F2 Atom	F1 Atom	F2 (ppm)	F1 (ppm)	No.	F2 Atom	F1 Atom	F2 (ppm)	F1 (ppm)
1	6	6	3.66	3.66	3	11	6	1.83	3.67
2	10	6	1.83	3.67	4	16	6	7.82	3.66

dx.doi.org/10.1021/jm300041e | J. Med. Chem. 2012, 55, 4244−4273

Table 8. continued

No.	F2 Atom	F1 Atom	F2 (ppm)	F1 (ppm)	No.	F2 Atom	F1 Atom	F2 (ppm)	F1 (ppm)
5	19	6	6.54	3.65	31	19	19	6.54	6.55
6	20	6	6.97	3.66	32	24	19	7.78	6.54
7	22	6	6.97	3.66	33	6	20	3.66	6.98
8	23	6	6.54	3.65	34	16	20	7.82	6.99
9	7	7	3.61	3.63	35	20	20	6.98	7
10	10	7	1.83	3.6	36	6	22	3.66	6.98
11	11	7	1.83	3.6	37	16	22	7.82	6.99
12	13	7	3.39	3.63	38	22	22	6.98	7
13	19	7	6.54	3.65	39	6	23	3.66	6.55
14	23	7	6.54	3.65	40	7	23	3.61	6.54
15	6	10	3.66	1.83	41	16	23	7.83	6.56
16	7	10	3.61	1.83	42	23	23	6.54	6.55
17	10	10	1.84	1.84	43	28	23	7.78	6.54
18	6	11	3.66	1.83	44	19	24	6.55	7.79
19	7	11	3.61	1.83	45	19	24	6.54	7.85
20	11	11	1.84	1.84	46	24	24	7.78	7.77
21	7	13	3.61	3.41	47	25	24	7.14	7.77
22	13	13	3.4	3.35	48	24	25	7.79	7.14
23	6	16	3.66	7.83	49	25	25	7.13	7.13
24	7	16	3.61	7.83	50	27	27	7.13	7.13
25	16	16	7.82	7.83	51	28	27	7.79	7.14
26	20	16	6.98	7.84	52	23	28	6.55	7.79
27	22	16	6.98	7.84	53	23	28	6.54	7.85
28	6	19	3.66	6.55	54	27	28	7.14	7.77
29	7	19	3.61	6.54	55	28	28	7.78	7.77
30	16	19	7.83	6.56					

LC-MS: (ES, m/z) $[M + H]^+$ calcd for $C_{27}H_{32}F_2N_5O_3$, 512; found, 512.

The Boc compound was treated with 20% TFA in CH_2Cl_2 (50 mL) and was added to the mixture. After the completion of this reaction (monitored by LCMS), the resulting mixture was concentrated under reduced pressure. The resulting residue was purified by reverse phase HPLC to yield product as a TFA salt. The acetonitrile−water layer was concentrated in vacuo to remove all the solvents. The residue was dissolved in dichloromethane and carefully neutralized by satd $NaHCO_3$. The organic layer was successively washed with brine followed by water. The organic layer was concentrated to yield **22** (450 mg, 52%). LC-MS: (ES, m/z) $[M + H]^+$ calcd for $C_{22}H_{23}F_2N_5O$, 412.2; found, 412.1. ^{1}H NMR (MeOH-d_4, 400 Hz) δ 7.61−7.57 (m, 2H), 6.94 (t, J = 8.8 Hz, 2H), 6.81 (t, J = 8.8 Hz, 2H), 6.47 (m, 2H), 3.72 (m, 2H), 3.58 (m, 2H), 3.42 (m, 2H), 1.85 (s, 6H). Elemental analysis compound **22** with 0.65 equiv H_2O: C, 62.44; N, 16.55; H,

dx.doi.org/10.1021/jm300041e | J. Med. Chem. 2012, 55, 4244−4273

5.79 (calculated). C = 62.54/62.44; N = 16.35/16.29; H = 5.52/5.61 (experimental).

The regiochemistry of the diMe groups was unambiguously assigned using 2-D NMR techniques (Table 8).

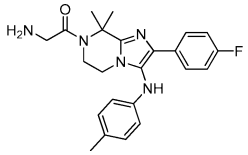

Synthesis of ***23****.* 2-Amino-1-(2-(4-fluorophenyl)-8,8-dimethyl-3-(*p*-tolylamino)-5,6-dihydroimidazo[1,2-*a*]pyrazin-7(8*H*)-yl)-ethanone:

Compound **23** was prepared from compound **10** (R_1 = Me, R_2 = Me) by a $Pd_2(dba)_3$ mediated amination reaction with 4-methylaniline followed by a TFA mediated deprotection in a protocol similar to compound **22**. ^{1}H NMR (MeOH-d_4, 400 MHz) δ 7.79−7.69 (m, 2H), 7.21 (t, J = 8.4 Hz, 2H), 7.04 (d, J = 8.0 Hz, 2H), 6.76 (d, J = 8.2 Hz, 2H), 4.11 (s, 2H), 3.88 (m, 4H), 2.22 (s, 3H), 2.12 (s, 6H). LC/MS major mass: 408.1 (M + H).

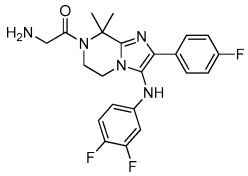

Synthesis of ***24****.* 2-Amino-1-(3-((3,4-difluorophenyl)amino)-2-(4-fluorophenyl)-8,8-dimethyl-5,6-dihydroimidazo[1,2-*a*]pyrazin-7(8*H*)-yl)ethanone:

Compound **24** was prepared from compound **10** (R_1= Me, R_2 = Me) by a $Pd_2(dba)_3$ mediated amination reaction with 3,4-difluoroaniline followed by a TFA mediated deprotection in a protocol similar to compound **22**. ^{1}H NMR (MeOH-d_4, 400 MHz) δ 7.73−7.69 (m, 2H), 7.21 (t, J = 8.8 Hz, 2H), 7.06−7.03 (m, 1H), 6.76−6.65 (m, 1H), 6.53−6.51 (m, 1H), 4.08−4.06 (m, 4H), 3.86−3.83 (m, 2H), 2.07 (s, 6H). Elemental analysis (compound +2.9 HCl): %C, 49.37; %H, 4.69; %N, 13.09; (calc). %C = 49.43/49.06; %N = 12.89/12.77; %H = 4.7/4.81 (experimental). m/z = 430.2 (M + 1).

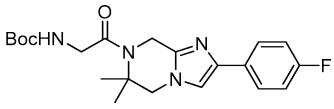

Synthesis of ***13****.* *tert*-Butyl 2-(3-bromo-2-(4-fluorophenyl)-6,6-dimethyl-5,6-dihydroimidazo [1,2-*a*]pyrazin-7(8*H*)-yl)-2-oxoethylcarbamate.

13 was prepared from compound **5a** by the following way:

To a stirred solution of compound **5a** (1.1 g, 3.38 mmol, 1.00 equiv) in DMF (30 mL) was added 3-chloro-2-methylprop-1-ene (500 mg, 5.49 mmol, 1.50 equiv), potassium carbonate (560 mg, 4.06 mmol, 1.10 equiv), and potassium iodide (1.12 g, 6.75 mmol, 2.00 equiv) at rt. The reaction mixture was stirred for 48 h at 40 °C. The reaction mixture was diluted with ethyl acetate (100 mL). The mixture was washed with brine (3 × 10 mL), dried over sodium sulfate, and concentrated under vacuum. The residue was applied onto a silica gel column with petroleum ether/EtOAc (5:1) to give 0.7 g (55%) of compound **5a-1** as a light-yellow solid. m/z = 380 (M + 1).

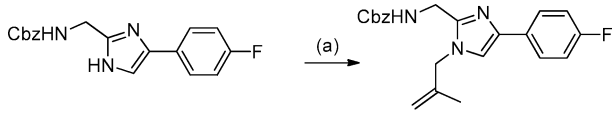

5a **5a-1**

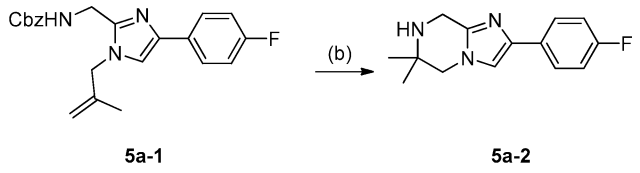

5a-1 **5a-2**

Into a 30 mL sealed tube, was placed compound **5a-1** (2.0 g, 5.28 mmol, 1.00 equiv), acetic acid (12 mL), and methanesulfonic acid (2 mL). The reaction mixture was stirred for 12 h at 260 °C (the temperature of the sand bath). The reaction mixture was cooled to rt. The mixture was poured into 20 mL of water. The aqueous layer was washed with ethyl acetate (3 × 10 mL). Aqueous sodium hydroxide (1N) was added to adjust pH to 8. The aqueous layer was extracted with ethyl acetate (3 × 10 mL). The combined organic layers were washed with brine (3 × 10 mL), dried over sodium sulfate, and concentrated under vacuum. The solid was collected by filtration and washed with 5 mL of *n*-hexane to give 500 mg (39%) of compound **5a-2** as a white solid. ^{1}H NMR (400 MHz, $CDCl_3$) δ 7.70−7.65 (m, 2H), 7.04−6.9 (m, 2H), 6.96 (s, 1H), 4.12 (s, 2H), 3.69 (s, 2H), 1.23 (s, 6H).

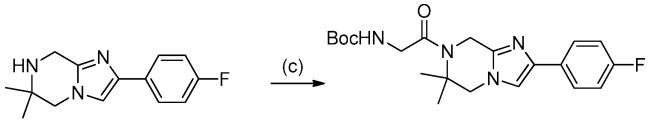

5a-2 **13**

To a stirred solution of compound **5a-2** (280 mg, 1.14 mmol, 1.0 equiv) in DMF (10 mL) was added 2-(*tert*-butoxycarbonyl)-acetic acid (600 mg, 3.43 mmol, 3.0 equiv), HATU (1.3 g, 3.42 mmol, 3.0 equiv), and DIEA (880 mg, 6.82 mmol, 6.0 equiv) at rt. The reaction mixture was stirred overnight at rt. The reaction mixture was diluted with ethyl acetate (100 mL). The organic layer was washed with brine (3 × 10 mL), dried over sodium sulfate, and concentrated under vacuum. The residue was applied onto a silica gel column with CH_2Cl_2/MeOH (10:1) to give 280 mg (57%) of compound **13** as a brown solid. ^{1}H NMR (400 MHz, $CDCl_3$) δ 7.72−7.68 (m, 2H), 7.23 (s, 1H), 7.13−7.07 (m, 2H), 5.46 (s, NH), 4.65 (s, 2H), 4.05−4.04 (m, 2H), 3.97 (s, 2H), 1.55−1.39 (m, 15H).

The structure of **13** was verified by HMQC, COSY, HMBC, and ROESY (Table 9).

Synthesis of ***25*** *(Analogue of Compound* ***14*** *in Scheme 3).* 2-Amino-1-(2-(4-fluorophenyl)-3-(4-fluorophenylamino)-6,6-dimethyl-5,6-dihydroimidazo[1,2-*a*]pyrazin-7(8*H*)-yl)-ethanone:

To a stirred solution of compound **13** (386 g, 0.96 mmol) in 6 mL of dichloromethane was added Br_2 (55 μL, 1.06 mmol) in acetic acid (2 mL). The reaction mixture was stirred at rt for 30 min. Solvent was removed via rotavap at a temperature no higher than 20 °C. After neutralization, the residue was subjected to flash chromatography (40 g, 0−100% ethyl acetate in hexane, 50 min, dry loading) purification to give 256 mg (55%) of the title compound **13a** as a colorless oil. ^{1}H NMR (400 MHz, $CDCl_3$) δ 7.87−7.83 (m, 2H), 7.03 (t, J = 8.8 Hz, 2H), 5.46 (s, 1H), 4.5 (s, 2H), 3.97 (d, J = 4.2 Hz, 2H), 3.81 (s, 2H), 1.45 (s, 6H), 1.39 (s, 9H).

dx.doi.org/10.1021/jm300041e | *J. Med. Chem.* 2012, 55, 4244−4273

Table 9. Structure of 13 Verified by HMQC, COSY, HMBC, and ROESY

^{1}H NMR (400 MHz, DMSO-d_6) δ ppm 1.36 (s, 6 H) 1.39 (s, 10 H) 3.85 (d, J=5.62 Hz, 2 H) 4.06 (s, 2 H) 4.60 (s, 2 H) 6.81 (br. s., 1 H) 7.18 (t, J=8.68 Hz, 2 H) 7.69 (s, 1 H) 7.75 - 7.81 (m, 2 H)

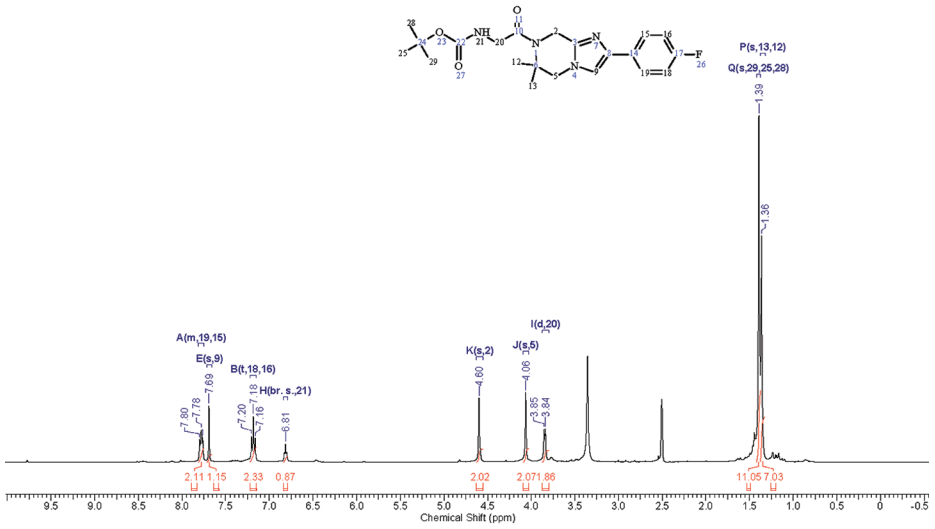

No.	Atom	Exp. Shift (ppm)	Multiplet	No.	Atom	Exp. Shift (ppm)	Multiplet
1	2	4.6	K	8	18	7.18	B
2	5	4.06	J	9	19	7.79	A
3	9	7.69	E	10	20	3.85	I
4	12	1.36	P	11	21	6.81	H
5	13	1.36	P	12	25	1.39	Q
6	15	7.79	A	13	28	1.39	Q
7	16	7.18	B	14	29	1.39	Q

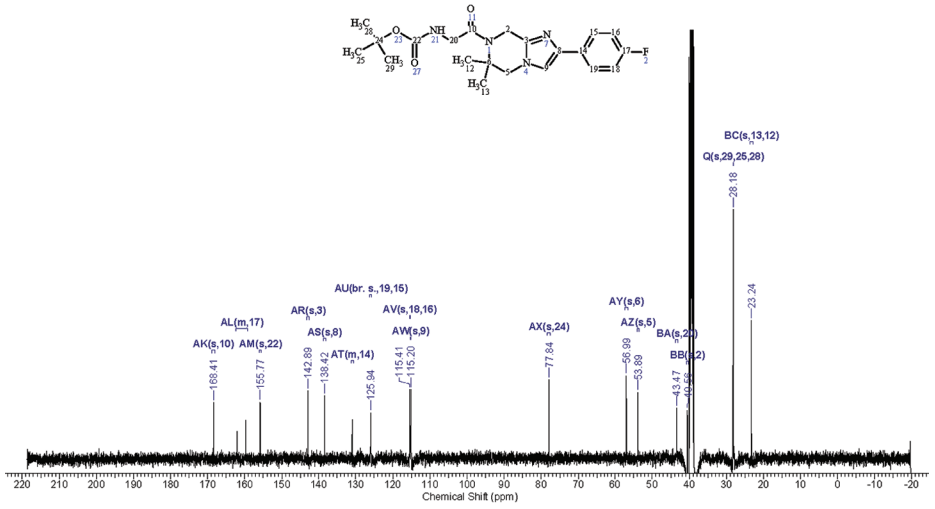

No.	Atom	Exp. Shift (ppm)	Multiplet	No.	Atom	Exp. Shift (ppm)	Multiplet
1	2	40.56	BB	3	5	53.89	AZ
2	3	142.89	AR	4	6	56.99	AY

dx.doi.org/10.1021/jm300041e | J. Med. Chem. 2012, 55, 4244−4273

Table 9. continued

No.	Atom	Exp. Shift (ppm)	Multiplet	No.	Atom	Exp. Shift (ppm)	Multiplet
5	8	138.42	AS	14	18	115.41	AV
6	9	115.2	AW	15	19	125.94	AU
7	10	168.41	AK	16	20	43.47	BA
8	12	23.24	BC	17	22	155.77	AM
9	13	23.24	BC	18	24	77.84	AX
10	14	130.93	AT	19	25	28.18	Q
11	15	125.94	AU	20	28	28.18	Q
12	16	115.41	AV	21	29	28.18	Q
13	17	160.78	AL				

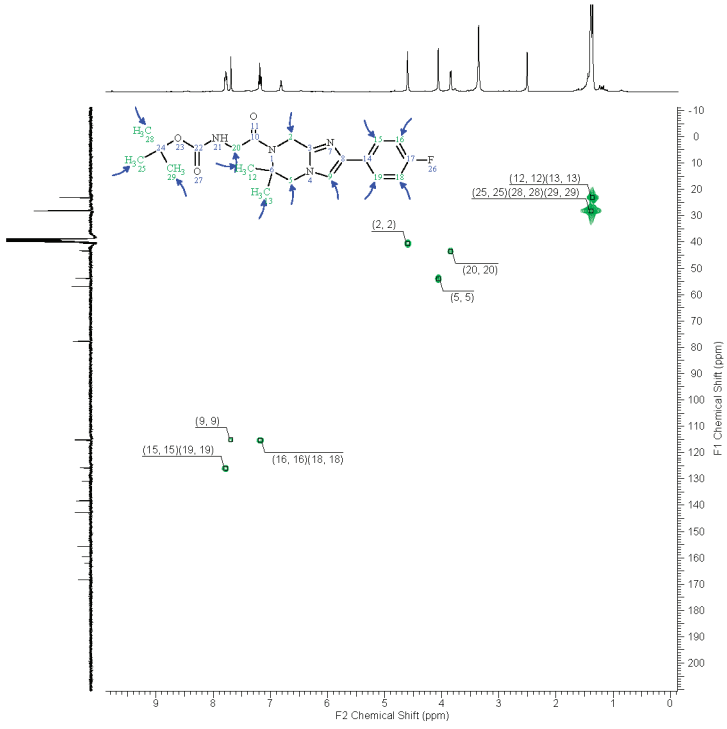

No.	F2 Atom	F1 Atom	F2 (ppm)	F1 (ppm)	No.	F2 Atom	F1 Atom	F2 (ppm)	F1 (ppm)
1	2	2	4.6	40.56	8	18	18	7.18	115.38
2	5	5	4.06	53.91	9	19	19	7.79	125.97
3	9	9	7.69	115.16	10	20	20	3.85	43.5
4	12	12	1.36	23.16	11	25	25	1.39	28.18
5	13	13	1.36	23.16	12	28	28	1.39	28.18
6	15	15	7.79	125.97	13	29	29	1.39	28.18
7	16	16	7.18	115.38					

dx.doi.org/10.1021/jm300041e | J. Med. Chem. 2012, 55, 4244−4273

Table 9. continued

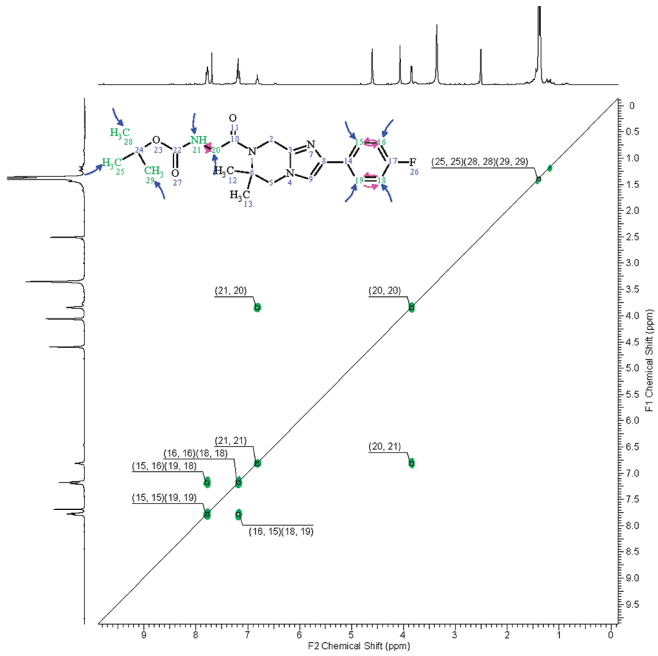

No.	F2 Atom	F1 Atom	F2 (ppm)	F1 (ppm)	No.	F2 Atom	F1 Atom	F2 (ppm)	F1 (ppm)
1	15	15	7.79	7.79	9	20	20	3.85	3.85
2	16	15	7.18	7.79	10	21	20	6.81	3.85
3	15	16	7.79	7.18	11	20	21	3.85	6.81
4	16	16	7.18	7.18	12	21	21	6.81	6.81
5	18	18	7.18	7.18	13	25	25	1.39	1.39
6	19	18	7.79	7.18	14	28	28	1.39	1.39
7	18	19	7.18	7.79	15	29	29	1.39	1.39
8	19	19	7.79	7.79					

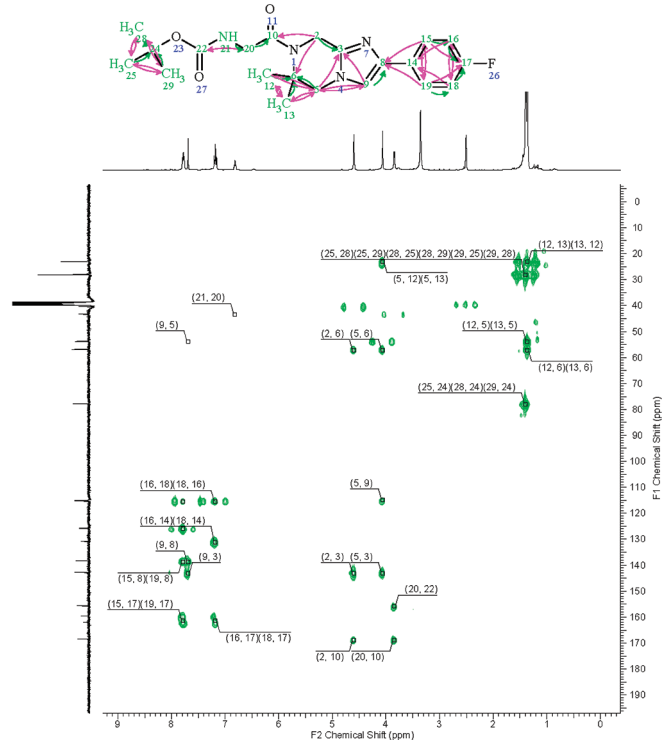

dx.doi.org/10.1021/jm300041e | J. Med. Chem. 2012, 55, 4244−4273

Table 9. continued

No.	F2 Atom	F1 Atom	F2 (ppm)	F1 (ppm)	No.	F2 Atom	F1 Atom	F2 (ppm)	F1 (ppm)
1	2	3	4.6	143.21	22	18	14	7.18	131.16
2	5	3	4.06	143.21	23	19	15	7.79	125.97
3	9	3	7.69	143.21	24	15	16	7.79	115.38
4	9	5	7.69	53.91	25	18	16	7.18	115.38
5	12	5	1.36	53.91	26	15	17	7.79	161.42
6	13	5	1.36	53.91	27	16	17	7.18	161.42
7	2	6	4.6	57.29	28	18	17	7.18	161.42
8	5	6	4.06	57.29	29	19	17	7.79	161.42
9	12	6	1.36	57.29	30	16	18	7.18	115.38
10	13	6	1.36	57.29	31	19	18	7.79	115.38
11	9	8	7.69	138.7	33	21	20	6.81	43.5
12	15	8	7.79	138.7	34	20	22	3.85	155.84
13	19	8	7.79	138.7	35	25	24	1.39	77.91
14	5	9	4.06	114.89	36	28	24	1.39	77.91
15	2	10	4.6	168.77	37	29	24	1.39	77.91
16	20	10	3.85	168.77	38	28	25	1.39	28.18
17	5	12	4.06	23.16	39	29	25	1.39	28.18
18	13	12	1.36	23.16	40	25	28	1.39	28.18
19	5	13	4.06	23.16	41	29	28	1.39	28.18
20	12	13	1.36	23.16	42	25	29	1.39	28.18
21	16	14	7.18	131.16	43	28	29	1.39	28.18

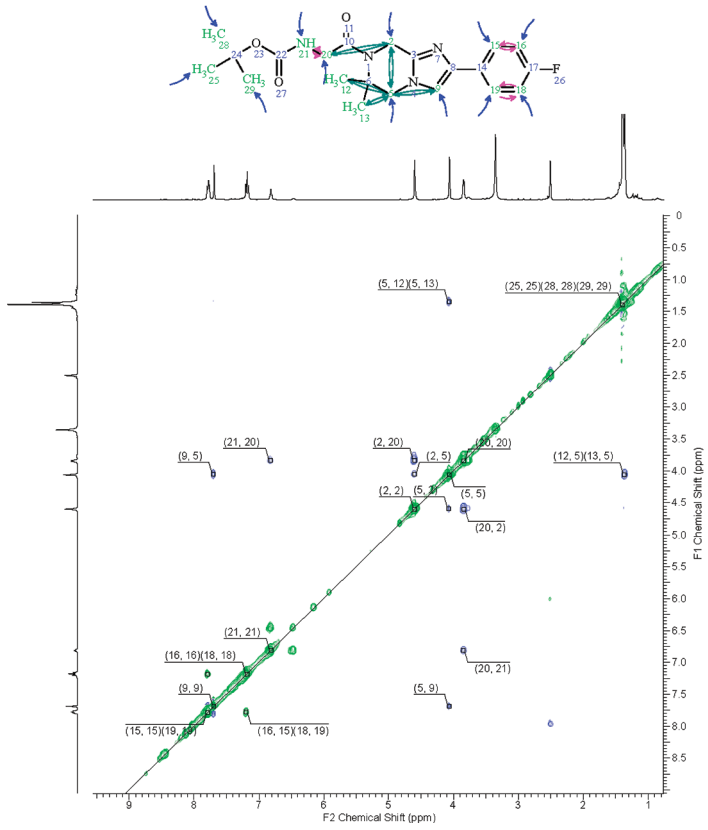

dx.doi.org/10.1021/jm300041e | J. Med. Chem. 2012, 55, 4244−4273

Table 9. continued

No.	F2 Atom	F1 Atom	F2 (ppm)	F1 (ppm)	No.	F2 Atom	F1 Atom	F2 (ppm)	F1 (ppm)
1	2	2	4.6	4.6	15	15	16	7.79	7.19
2	5	2	4.07	4.59	16	16	16	7.18	7.18
3	20	2	3.85	4.6	17	18	18	7.18	7.18
4	2	5	4.6	4.05	18	19	18	7.79	7.19
5	5	5	4.06	4.06	19	18	19	7.2	7.78
6	9	5	7.7	4.05	20	19	19	7.79	7.79
7	12	5	1.37	4.06	21	2	20	4.6	3.83
8	13	5	1.37	4.06	22	20	20	3.85	3.85
9	5	9	4.06	7.69	23	21	20	6.82	3.84
10	9	9	7.69	7.69	24	20	21	3.85	6.81
11	5	12	4.07	1.35	25	21	21	6.81	6.81
12	5	13	4.07	1.35	26	25	25	1.39	1.39
13	15	15	7.79	7.79	27	28	28	1.39	1.39
14	16	15	7.2	7.78	28	29	29	1.39	1.39

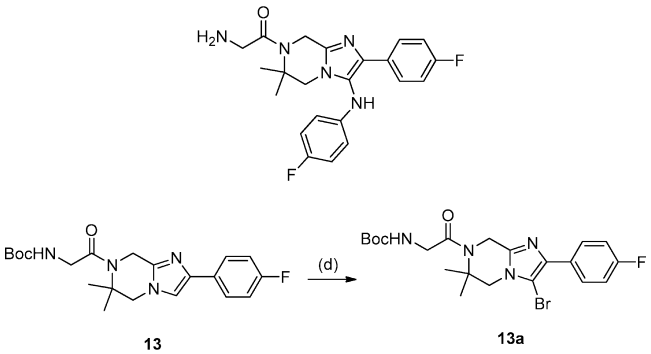

13 **13a**

Example **25** was obtained from **13a** by a $Pd_2(dba)_3$ mediated amination reaction with 4-fluoroaniline followed by a TFA mediated deprotection by analogy to compound **22** (55% yield over 2 steps). ^{1}H NMR (400 MHz, DMSO-d_6): δ 8.06 (m, 2H), 7.98 (m, 1H), 7.80 (m, 2H), 7.16 (m, 2H), 6.98 (m, 2H), 6.60 (m, 2H), 4.64 (m, 2H), 4.02 (m, 2H), 3.80 (m, 2H), 1.38 (s, 6H). m/z = 412.1 (M + 1).

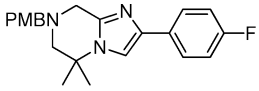

7b

Synthesis of ***7b***. 2-(4-Fluorophenyl)-7-(4-methoxybenzyl)-5,5-dimethyl-5,6,7,8-tetrahydroimidazo[1,2-*a*]pyrazine:

Compound **7b** was prepared from compound **7a** (R_1 = R_2 = H) by the following way:

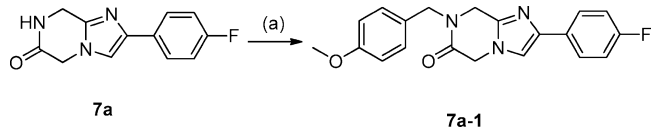

7a **7a-1**

To a solution of compound **7a** (231 mg, 1.0 mmol) in DMF (10 mL) were added KOH (168 mg, 3.0 mmol) and PMBCl (405 μL, 3.0 mmol) at 0 °C. The reaction mixture was stirred at the same temperature for 2 h and at rt for 2 additional hours. The reaction mixture was purified by reverse phase HPLC. The HPLC fraction were evaporated under reduced pressure and neutralized by satd $NaHCO_3$. The compound was extracted by ethyl acetate and dried over sodium sulfate. The organic layer was concentrated under reduced pressure to give compound **7a-1** (221 mg, 63%) as a white solid. ^{1}H NMR (400 MHz, $CDCl_3$) δ 7.67−7.63 (m, 2H), 7.28−7.25 (m, 2H), 7.07−7.02 (m, 2H), 6.89−6.86 (m, 2H), 4.74 (s, 2H), 4.70 (m, 2H), 4.53 (s, 2H), 3.79 (s, 3H).

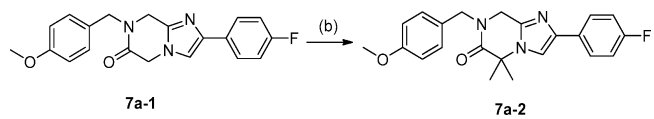

7a-1 **7a-2**

To a solution of compound **7a-1** (253 mg, 0.72 mmol) in DMF (15 mL) were added 60% sodium hydride (87 mg, 0.085 mmol) and methyl iodide (0.45 mL, 7.2 mmol) at rt. The reaction mixture was stirred at rt for 2 h. The reaction mixture was quenched with methanol and directly subjected to mass-triggered HPLC purification to give **7a-2** as a white solid after evaporation of

dx.doi.org/10.1021/jm300041e | *J. Med. Chem.* 2012, 55, 4244−4273

Table 10. Structure of 7a-2 Verified by 2-D NMR Techniques

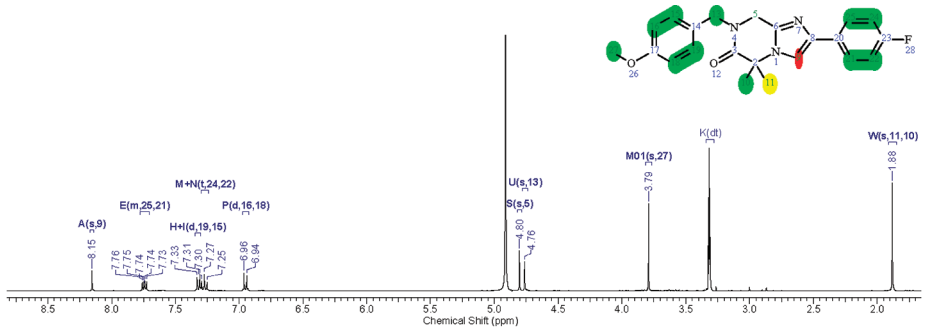

No.	Atom	Exp. Shift (ppm)	Calc. Shift (ppm)	Difference (ppm)	Multiplet	No.	Atom	Exp. Shift (ppm)	Calc. Shift (ppm)	Difference (ppm)	Multiplet
1	5	4.8	-	-	S	9	16	6.95	6.83	0.121	P
2	5	-	4.176	-	-	10	18	6.95	6.83	0.121	P
3	5	-	4.176	-	-	11	19	7.32	7.248	0.071	H+I
4	9	8.15	6.742	1.412	A	12	21	7.74	7.46	0.283	E
5	10	1.88	1.798	0.084	W	13	22	7.27	7.039	0.234	M+N
6	11	1.88	1.421	0.461	W	14	24	7.27	7.039	0.234	M+N
7	13	4.76	4.62	0.143	U	15	25	7.74	7.46	0.283	E
8	15	7.32	7.248	0.071	H+I	16	27	3.79	3.83	0.038	M01

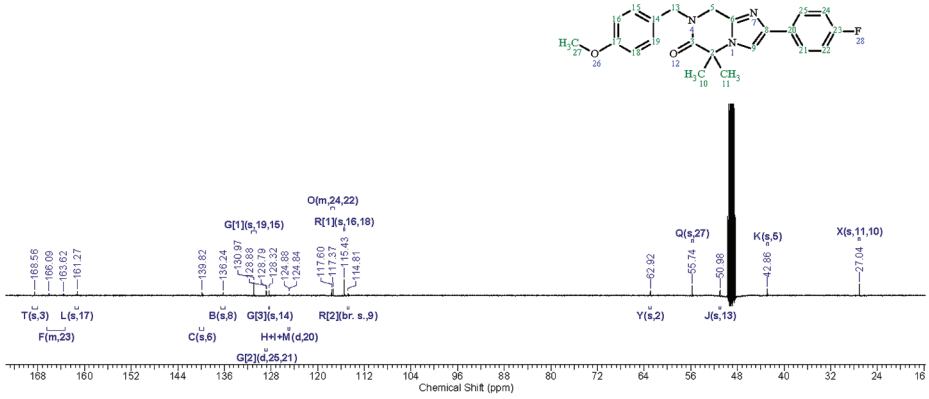

No.	Atom	Exp. Shift (ppm)	Multiplet	No.	Atom	Exp. Shift (ppm)	Multiplet
1	2	62.92	Y	12	16	115.43	R[1]
2	3	168.56	T	13	17	161.27	L
3	5	42.86	K	14	18	115.43	R[1]
4	6	139.82	C	15	19	130.97	G[1]
5	8	136.24	B	16	20	124.86	H+I+M
6	9	114.81	R[2]	17	21	128.84	G[2]
7	10	27.04	X	18	22	117.48	O
8	11	27.04	X	19	23	164.86	F
9	13	50.98	J	20	24	117.48	O
10	14	128.32	G[3]	21	25	128.84	G[2]
11	15	130.97	G[1]	22	27	55.74	Q

dx.doi.org/10.1021/jm300041e | J. Med. Chem. 2012, 55, 4244−4273

Table 10. continued

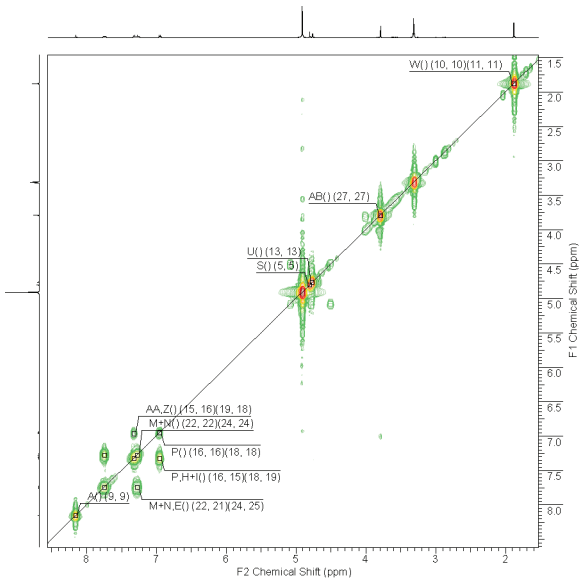

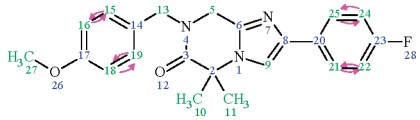

No.	F2 Atom	F1 Atom	F2 (ppm)	F1 (ppm)	No.	F2 Atom	F1 Atom	F2 (ppm)	F1 (ppm)
1	5	5	4.8	4.8	12	18	19	6.95	7.32
2	9	9	8.15	8.15	13	19	19	7.32	7.32
3	10	10	1.88	1.88	14	21	21	7.74	7.74
4	11	11	1.88	1.88	15	22	21	7.27	7.74
5	13	13	4.76	4.76	16	21	22	7.74	7.27
6	15	15	7.32	7.32	17	22	22	7.27	7.27
7	16	15	6.95	7.32	18	24	24	7.27	7.27
8	15	16	7.32	6.96	19	25	24	7.74	7.27
9	16	16	6.95	6.95	20	24	25	7.27	7.74
10	18	18	6.95	6.95	21	25	25	7.74	7.74
11	19	18	7.32	6.96	22	27	27	3.79	3.8

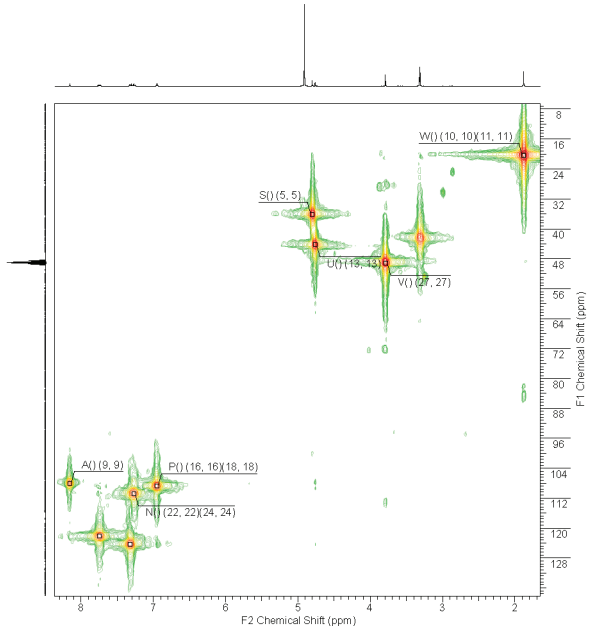

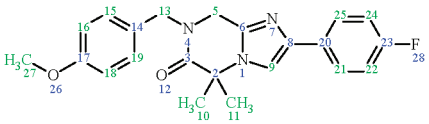

dx.doi.org/10.1021/jm300041e | J. Med. Chem. 2012, 55, 4244−4273

Table 10. continued

No.	F2 Atom	F1 Atom	F2 (ppm)	F1 (ppm)	No.	F2 Atom	F1 Atom	F2 (ppm)	F1 (ppm)
1	5	5	4.8	36.13	9	18	18	6.95	108.76
2	9	9	8.15	108.09	10	19	19	7.32	124.31
3	10	10	1.88	20.31	11	19	19	7.32	124.33
4	11	11	1.88	20.31	12	21	21	7.74	122.18
5	13	13	4.76	44.27	13	22	22	7.27	110.83
6	15	15	7.32	124.31	14	24	24	7.27	110.83
7	15	15	7.32	124.33	15	25	25	7.74	122.18
8	16	16	6.95	108.76	16	27	27	3.79	49.12

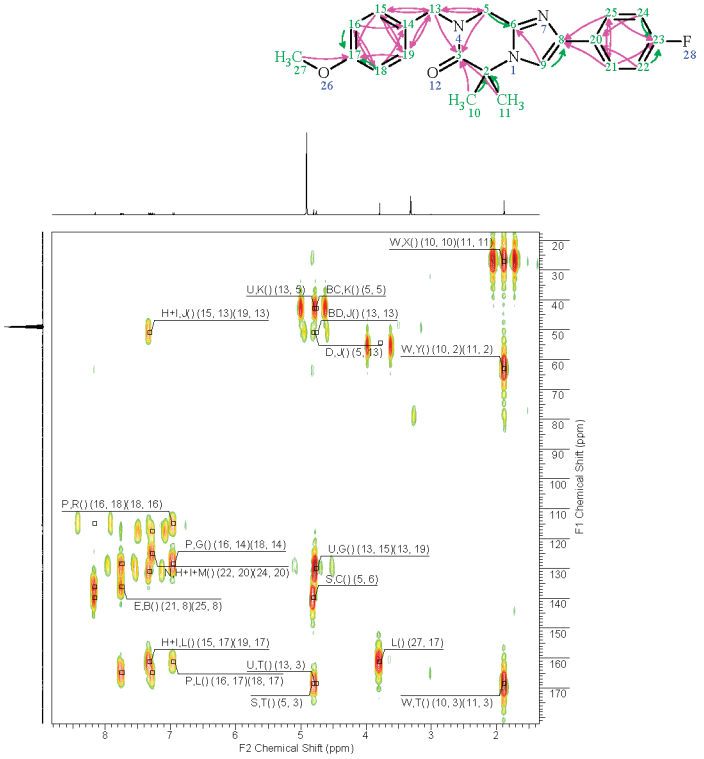

No.	F2 Atom	F1 Atom	F2 (ppm)	F1 (ppm)	No.	F2 Atom	F1 Atom	F2 (ppm)	F1 (ppm)
1	10	2	1.88	62.92	10	9	6	8.16	139.82
2	11	2	1.88	62.92	11	9	8	8.16	136.24
3	5	3	4.8	168.56	12	21	8	7.74	136.24
4	10	3	1.88	168.56	13	25	8	7.74	136.24
5	11	3	1.88	168.56	14	9	9	8.16	114.81
6	13	3	4.76	168.56	15	10	10	1.88	27.04
7	5	5	4.79	42.86	16	11	11	1.88	27.04
8	13	5	4.76	42.86	17	5	13	4.8	50.98
9	5	6	4.8	139.82	18	13	13	4.76	50.98

dx.doi.org/10.1021/jm300041e | J. Med. Chem. 2012, 55, 4244−4273

Table 10. continued

No.	F2 Atom	F1 Atom	F2 (ppm)	F1 (ppm)	No.	F2 Atom	F1 Atom	F2 (ppm)	F1 (ppm)
19	15	13	7.32	50.98	34	15	19	7.32	130.97
20	19	13	7.32	50.98	35	19	19	7.32	130.97
21	16	14	6.95	128.32	36	22	20	7.27	124.86
22	18	14	6.95	128.32	37	24	20	7.27	124.86
23	13	15	4.76	129.84	38	21	21	7.74	128.32
24	15	15	7.32	130.97	39	25	21	7.74	128.32
25	19	15	7.32	130.97	40	22	22	7.27	117.48
26	18	16	6.95	114.81	41	21	23	7.74	164.86
27	15	17	7.32	161.27	42	22	23	7.27	164.86
28	16	17	6.95	161.27	43	24	23	7.27	164.86
29	18	17	6.95	161.27	44	25	23	7.74	164.86
30	19	17	7.32	161.27	45	24	24	7.27	117.48
31	27	17	3.79	161.27	46	21	25	7.74	128.32
32	16	18	6.95	114.81	47	25	25	7.74	128.32
33	13	19	4.76	129.84	48	27	27	3.78	54.41

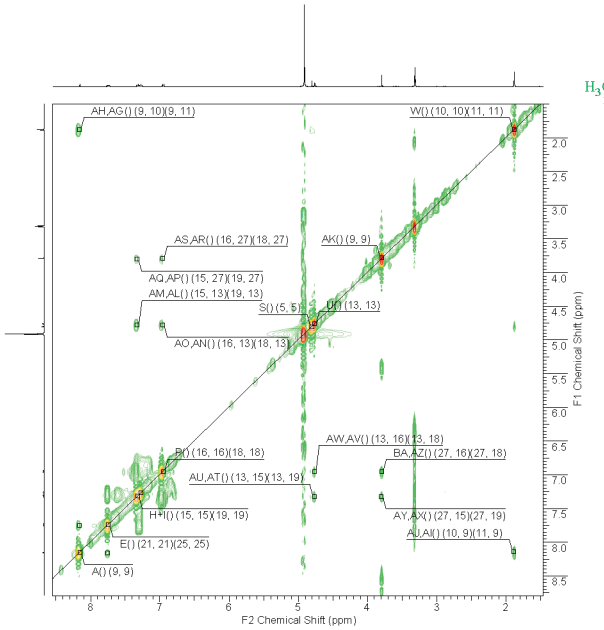

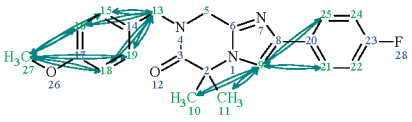

No.	F2 Atom	F1 Atom	F2 (ppm)	F1 (ppm)	No.	F2 Atom	F1 Atom	F2 (ppm)	F1 (ppm)
1	5	5	4.8	4.8	11	11	11	1.88	1.88
2	9	9	3.8	3.79	12	13	13	4.76	4.76
3	9	9	8.15	8.15	13	15	13	7.33	4.78
4	10	9	1.88	8.14	14	16	13	6.96	4.78
5	11	9	1.88	8.14	15	18	13	6.96	4.78
6	21	9	7.76	8.16	16	19	13	7.33	4.78
7	25	9	7.76	8.16	17	13	15	4.77	7.32
8	9	10	8.16	1.88	18	15	15	7.32	7.32
9	10	10	1.88	1.88	19	27	15	3.8	7.32
10	9	11	8.16	1.88	20	13	16	4.77	6.96

dx.doi.org/10.1021/jm300041e | J. Med. Chem. 2012, 55, 4244−4273

Table 10. continued

No.	F2 Atom	F1 Atom	F2 (ppm)	F1 (ppm)	No.	F2 Atom	F1 Atom	F2 (ppm)	F1 (ppm)
21	16	16	6.95	6.95	30	21	21	7.74	7.74
22	27	16	3.8	6.96	31	22	22	7.27	7.27
23	13	18	4.77	6.96	32	24	24	7.27	7.27
24	18	18	6.95	6.95	33	9	25	8.16	7.75
25	27	18	3.8	6.96	34	25	25	7.74	7.74
26	13	19	4.77	7.32	35	15	27	7.33	3.8
27	19	19	7.32	7.32	36	16	27	6.96	3.8
28	27	19	3.8	7.32	37	18	27	6.96	3.8
29	9	21	8.16	7.75	38	19	27	7.33	3.8

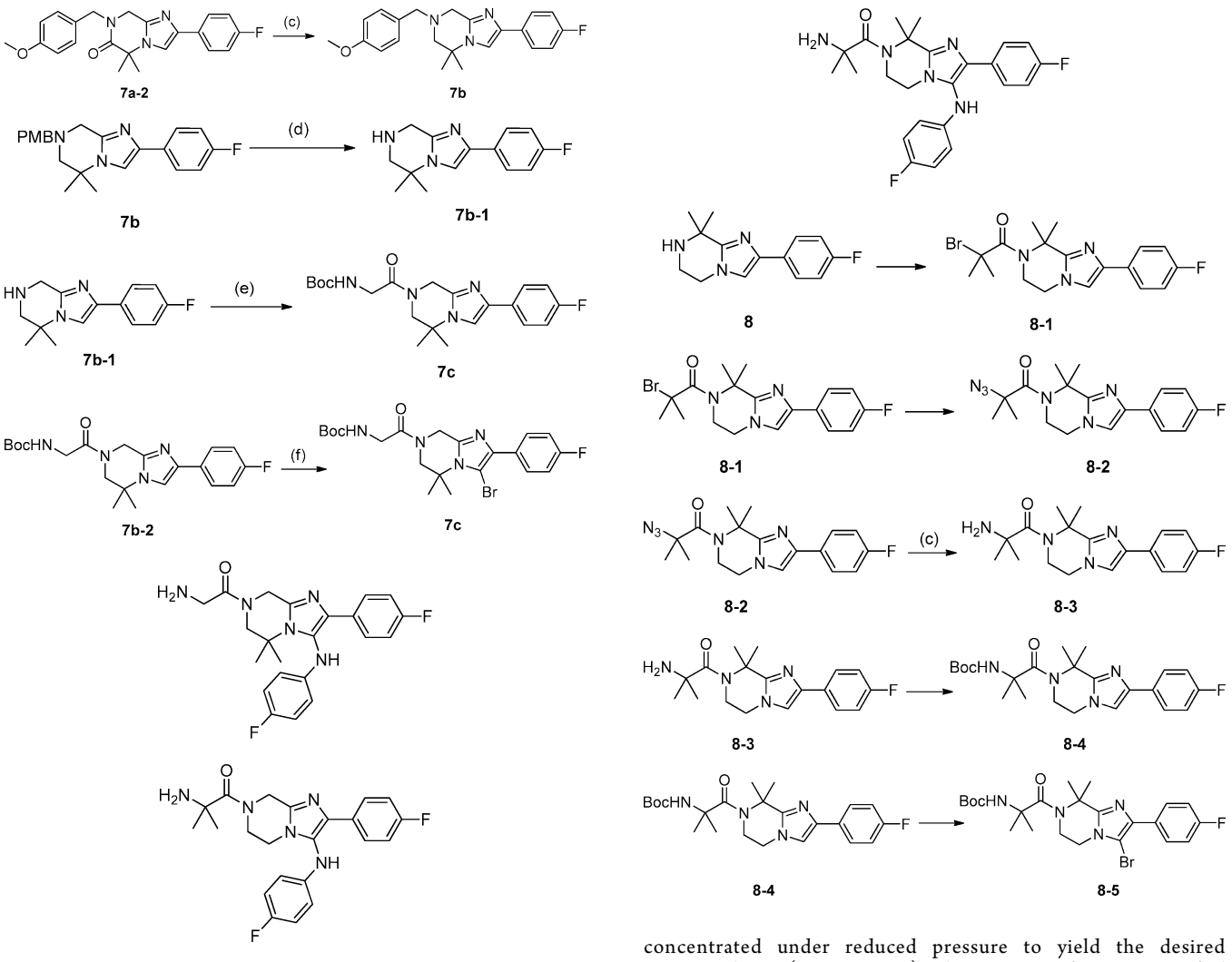

acetonitrile−water in vacuo. The TFA salt was subsequently neutralized by saturated sodium bicarbonate solution and extracted with dichloromethane to get the compound as a free base. The organic layer was dried over sodium sulfate and concentrated under reduced pressure to yield the desired compound **7a-2** (234 mg, 86%). The structure of **7a-2** was verified by 2-D NMR techniques (Table 10).

*Synthesis of Compound **7b**.* To a solution of compound **7a-2** (170 mg, 0.45 mmol) in THF (9 mL) was added 1.0 N BH_3·THF (2.70 mL, 2.70 mmol) at rt. The reaction mixture was stirred at reflux for 2 h.

dx.doi.org/10.1021/jm300041e | J. Med. Chem. 2012, 55, 4244−4273

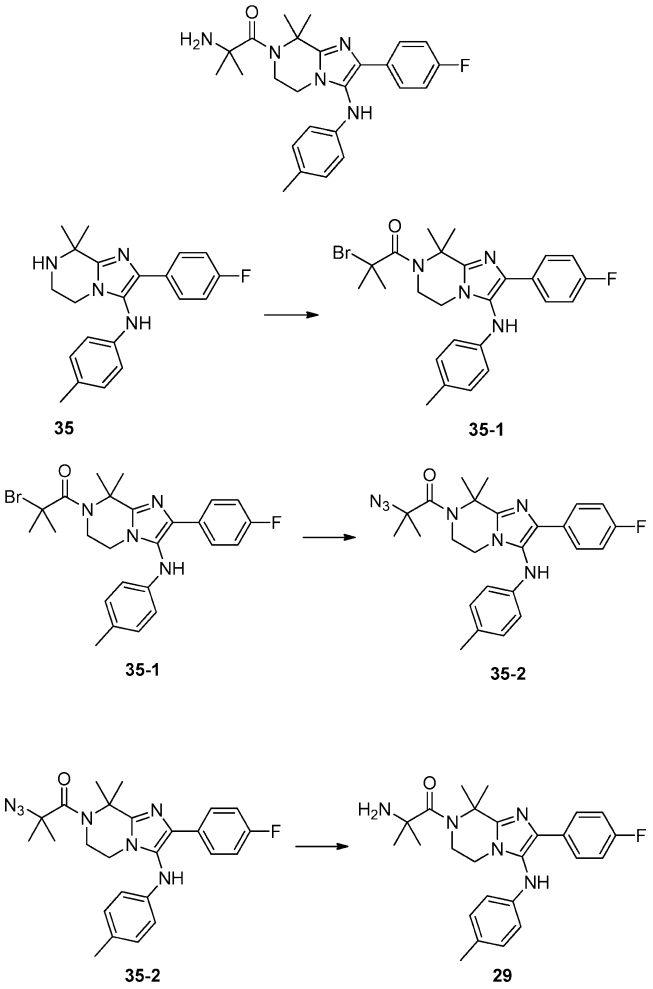

Pd/C was added (gas generated). The reaction mixture was stirred for 1 h. Solid was filtered off, and solvent was removed. The structure of crude compound **7b** was verified by proton NMR. The product was assumed to be of 100% yield and used in the next step without further purification. ^{1}H NMR (400 MHz, CD_3OD) δ 8.1 (s, 1H), 7.74–7.70 (m, 2H), 7.34 (d, J = 8.6 Hz, 2H), 7.27 (m, 2H), 6.94 (d, J = 8.6 Hz, 2H), 3.91 (s, 2H), 3.80 (s, 3H), 3.79 (s, 2H), 2.87 (s, 2H), 1.61 (s, 6H).

7-(4-Methoxybenzyl)-2-(4-fluorophenyl)-5,5-dimethyl-5,6,7,8-tetrahydroimidazo[1,2-*a*]pyrazine (1.07 g, 2.93 mmol, 1.00 equiv) (**7b**) was added to trifluoroacetic acid (15 mL). The resulting solution was stirred for 2 h at 70 °C in an oil bath. The resulting mixture was concentrated under vacuum. The residue was dissolved in 200 mL of dichloromethane. The pH value of the solution was adjusted to 8 with

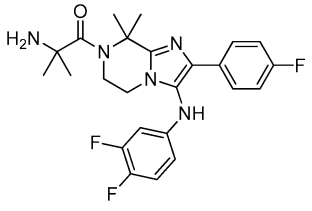

aqueous sodium bicarbonate. **7b-1** was extracted from the aqueous layer using 3 × 100 mL of ethyl acetate. The mixture was dried over sodium sulfate and concentrated under vacuum. This resulted in **7b-1** (718 mg, quantitative) as a yellow solid. m/z = 246 (M + H).

To a solution of **7b-1** (750 mg, 3.06 mmol, 1.00 equiv) in *N*,*N*-dimethylformamide (30 mL) were added 2-(*tert*-butoxycarbonyl)acetic acid (850 mg, 4.86 mmol, 1.50 equiv), HATU (1.3 g, 3.42 mmol, 1.10 equiv), and triethylamine (650 mg, 6.44 mmol, 2.00 equiv). The resulting solution was stirred overnight at rt. The residue was dissolved in ethyl acetate (200 mL). The resulting mixture was washed with brine (3 × 100 mL), dried over anhydrous sodium sulfate, and

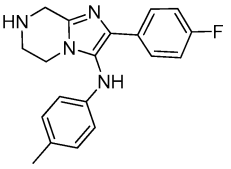

concentrated under vacuum. The residue was applied onto a silica gel column with petroleum ether/ethyl acetate (4:1). This resulted in 600 mg (49%) of **7c** as a pale-yellow solid. ^{1}H NMR (300 MHz, $CDCl_3$): δ 7.75 (m, 2H), 7.22 (s, 1H), 7.13–7.07 (m, 2H), 4.99–4.87 (m, 2H), 4.12 (s, 2H), 3.91 3.65 (m, 2H), 1.57 (m, 6H), 1.43 (s, 9H).

To a stirred solution of compound **7b-2** (583 g, 1.45 mmol) in dichloromethane (6 mL) was added Br_2 (82 μL, 1.60 mmol) in acetic acid (2 mL). The reaction mixture was stirred at rt for 30 min. Solvent was removed via rotavap at a temperature no higher than 20 °C. After neutralization, the residue was subjected to flash

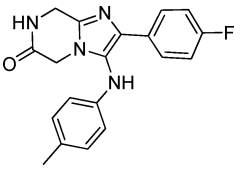

chromatography (40 g, 0–100% ethyl acetate in hexane, 50 min, dry loading) purification to give 628 mg (90%) of the title compound **7c** as a yellow solid. ^{1}H NMR (400 MHz, $CDCl_3$) δ 781–7.78 (m, 2H), 7.07 (t, J = 8.6 Hz, 2H), 5.28 (s, NH), 4.84–4.7 (m, 2H), 4.07–3.58 (m, 4H), 1.49–1.44 (m, 6H), 1.28 (s, 9H).

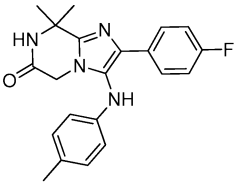

33

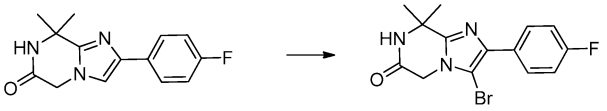

7 33a

Synthesis of ***26***. 2-Amino-1-(2-(4-fluorophenyl)-3-(4-fluorophenylamino)-5,5-dimethyl-5,6-dihydroimidazo[1,2-*a*]pyrazin-7(8*H*)-yl)-ethanone:

Compound **26** was prepared from compound **7c** by a $Pd_2(dba)_3$ mediated amination reaction with 4-fluoroaniline followed by a TFA mediated deprotection in 46% yield over 2 steps. ^{1}H NMR (400 MHz, CD_3OD): δ 7.57 (m, 2H), 7.02 (m, 2H), 6.77 (m, 2H), 6.52 (m, 2H), 4.97–4.91 (m, 2H), 4.09–3.74 (m, 4H), 1.56 (s, 3H), 1.51 (s, 3H). m/z = 412.2 (M + 1).

Synthesis of ***27***. 2-Amino-1-(2-(4-fluorophenyl)-3-((4-fluorophenyl)amino)-5,6-dihydroimidazo[1,2-*a*]pyrazin-7(8*H*)-yl)-2-methylpropan-1-one. The synthesis has been reported in the previous communication.[5]

Synthesis of ***28***. 2-Amino-1-(2-(4-fluorophenyl)-3-(4-fluorophenylamino)-8,8-dimethyl-5,6-dihydroimidazo[1,2-*a*]pyrazin-7(8*H*)-yl)-2-methylpropan-1-one:

dx.doi.org/10.1021/jm300041e | *J. Med. Chem.* 2012, 55, 4244–4273

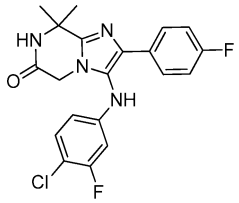

Compound **28** was prepared from compound **8** ($R_1 = R_2 = Me$) in the following fashion using a slightly modified route to the one described in Scheme 2.

To a stirred solution of compound **8** (1.48 g, 6.04 mmol) and NEt_3 (6.0 g, 59.4 mmol) in dichloromethane (20 mL) was added 2-bromo-2-methylpropanoyl bromide (14 g, 60.9 mmol) dropwise at rt. After being stirred for 3 h at rt, the reaction was then quenched by the addition of water (30 mL). The resulting solution was extracted with

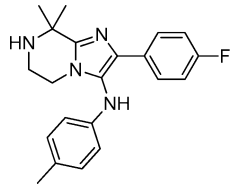

3 × 30 mL of ethyl acetate. The combined organic layers were washed with brine, dried over anhydrous sodium sulfate, and concentrated under vacuum. This resulted in crude product as a dark solid, which was washed with EtOAc:petroleum ether (1:10) to remove the impurities to produce compound **8-1** as a gray solid. *m/z* 396 (M + H).

To a solution of compound **8-1** (2.0 g, 5.08 mmol, 1.00 equiv) in DMF (10 mL) was NaN_3 (1.0 g, 15.38 mmol, 3.00 equiv) at rt. The

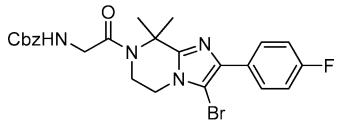

35-1

reaction mixture was stirred overnight at rt. The resulting solution was diluted with 300 mL of ethyl acetate. The resulting mixture was washed with 3 × 20 mL of brine, dried over anhydrous sodium sulfate,

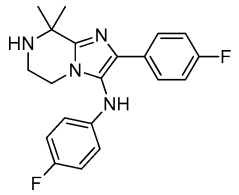

and concentrated under vacuum. The residue was applied onto a silica gel column with petroleum ether/EtOAc (5:1) to give compound **8-2** as a white solid. *m/z* 357 (M + H).

To a stirred solution of compound **8-2** (1.2 g, 3.37 mmol, 1.00 equiv) in methanol (20 mL) was added Pd/C (80 mg, 0.75 mmol, 0.20 equiv) at rt. The reaction mixture was evacuated and backfilled with H_2. The reaction mixture was stirred overnight at rt. The solids were filtered out. The resulting mixture was concentrated under vacuum. The solid was washed with petroleum ether. This resulted in compound **8-3** as a white solid. *m/z* 331 (M + H).

To a stirred solution of compound **8-3** (910 mg, 2.76 mmol, 1.00 equiv) in THF (50 mL) was added BOC anhydride (3.2 g, 14.68 mmol, 5.00 equiv), followed by aqueous NaOH (1N, 6 mL, 2.0 equiv) at rt. The resulting solution was stirred for 24 h at 40 °C. The resulting solution was concentrated under vacuum. The mixture was diluted with EtOAc (60 mL). The organic layer was washed with 3 × 10 mL of brine, dried over Na_2SO_4, and concentrated under vacuum. The solid was collected by filtration and washed with *n*-hexane (5 mL) to give compound **8-4** as a white solid. ^{1}H NMR (300 MHz, $CDCl_3$) δ 7.75−7.71 (m, 2H), 7.09−7.02 (m, 3H), 4.84(s, NH), 4.09−4.0 (m, 4H), 1.98 (s, 6H), 1.55 (s, 6H), 1.45 (s, 9H).

To a stirred solution of compound **8-4** (32 mg, 0.074 mmol) in dichloromethane (3 mL) was added Br_2 (4.2 μL, 0.082 mmol) in acetic acid (1 mL). The reaction mixture was stirred at rt for 30 min. Solvent was removed via rotavap at a temperature no higher than 20 °C. After neutralization, the residue was subjected to flash chromatography (4 g, 0−60% ethyl acetate in hexane, 16 min) purification to give the compound **8-5** as colorless oil, was collected by filtration, and washed with *n*-hexane (5 mL) to give compound **8-4** as a white solid. ^{1}H NMR (400 MHz, $CDCl_3$) δ 7.91−7.88 (m, 2H), 7.10−7.04 (m, 2H), 5.11(s, NH), 4.01 (m, 2H), 3.96 (s, 2H), 1.94 (s, 6H), 1.51 (s, 6H), 1.41 (s, 9H).

Compound **28** was prepared from compound **8-5** by a $Pd_2(dba)_3$ mediated amination reaction with 4-fluoroaniline followed by a TFA mediated deprotection. ^{1}H NMR (400 MHz, MeOH-d_4) δ 7.66 (dd, *J* = 9.2, 5.2 Hz, 2H), 7.11 (t, *J* = 8.8 Hz, 2H), 6.81 (t, *J* = 8.8 Hz, 2H), 6.72−6.68 (m, 2H), 4.04−3.99 (m, 4H), 2.01 (s, 6H), 1.66 (s, 6H). *m/z* = 440.1 (M + 1).

Synthesis of ***29***. 2-Amino-1-(2-(4-fluorophenyl)-8,8-dimethyl-3-(*p*-tolylamino)-5,6-dihydroimidazo[1,2-*a*]pyrazin-7(8*H*)-yl)-2-methylpropan-1-one:

Compound **29** was prepared from **35** by the following way:

To a stirred solution of **35** (21 mg, 0.06 mmol) and Et_3N (83 μL, 0.60 mmol) in dry dichloromethane (6 mL) was added 2-bromo-2-methylpropanoyl bromide (71 μL, 0.60 mmol). The reaction mixture was stirred at rt for 5 h. The reaction mixture was concentrated and subjected to mass-triggered LC/MS purification directly. The obtained solution was concentrated to give 22 mg (73%) of compound **35-1** as yellow oil after neutralization. ^{1}H NMR (400 MHz, MeOH-d_4) δ 7.71−7.66 (m, 2H), 7.23−7.19 (m, 2H), 7.02 (d, *J* = 8.4 Hz, 2H), 6.66 (d, *J* = 8.4 Hz, 2H), 4.31 (m, 2H), 4.09 (m, 2H), 2.21 (s, 3H), 2.06 (s, 6H), 2.00 (s, 6H).

To a solution of compound **35-1** (22 mg, 0.044 mmol) in DMF (3 mL) was added NaN_3 (8.6 mg, 0.132 mmol) at rt. The reaction mixture was stirred at rt for 2 h. The reaction mixture was directly subjected to mass-triggered HPLC purification directly. The obtained MeCN/aqueous solution was combined and concentrated to give 15 mg (75%) of compound **35-2** as yellow oil after neutralization. ^{1}H NMR (400 MHz, MeOH-d_4) δ 7.70 −7.66 (m, 2H), 7.23−7.19 (m, 2H), 7.04 (d, *J* = 8.3 Hz, 2H), 6.66 (d, *J* = 8.4 Hz, 2H), 4.26 (m, 2H), 4.07−4.05 (m, 2H), 2.24 (s, 3H), 2.03 (s, 6H), 1.58 (s, 6H).

To a solution of compound **35-2** (15 mg, 0.033 mmol) in MeOH (3 mL) was added 10% Pd/C (4 mg, 0.003 mmol) at rt. Air was removed, and H_2 was filled. The reaction mixture was stirred at rt for 2 h. Solid was filtered off, and solvent was removed. The reaction mixture was directly subjected to mass-triggered HPLC purification to give 15 mg (100%) of the title compound yellow oil. ^{1}H NMR (MeOH-d_4, 400 Hz) δ 7.78−7.75 (m, 2H), 7.06−6.97 (m, 4H), 6.56 (d, *J* = 8.4 Hz, 2H), 5.16 (s, NH), 4.33 (t, *J* = 4.8 Hz, 2H), 3.74 (t, *J* = 4.8 Hz, 2H), 2.29 (s, 3H), 1.95 (s, 6H), 1.45 (s, 6H). *m/z* = 436.2 (M + 1).

Synthesis of ***30***. 2-Amino-1-(3-(3,4-difluorophenylamino)-2-(4-fluorophenyl)-8,8-dimethyl-5,6-dihydroimidazo[1,2-*a*]pyrazin-7(8*H*)-yl)-2-methylpropan-1-one:

Compound **30** was prepared from compound **8-5** by a $Pd_2(dba)_3$ mediated amination reaction with 3,4-difluoroaniline followed by a TFA mediated deprotection.^{1}H NMR (400 MHz, MeOH-d_4) δ 7.63−7.60 (m, 2H), 7.14 (t, *J* = 8.4 Hz, 2H), 7.01 (dd, *J* = 18.8, 8.8 Hz, 1H), 6.68−6.63 (m, 1H), 6.5 (m, 1H), 4.03 (m, 2H), 4.01 (m, 2H), 2.01 (s, 6H), 1.66 (s, 6H). *m/z* = 458.1 (M + 1).

Synthesis of ***31***. 2-(4-Fluorophenyl)-*N*-(*p*-tolyl)-5,6,7,8-tetrahydroimidazo[1,2-*a*]pyrazin-3-amine:

The details of the synthesis involving an Ugi reaction between 4-fluorobenzaledehyde, 2-aminopyrazine, and 1-isocyano-4-methylbenzene has been reported in the previous communication.[5] ^{1}H NMR (400 MHz, MeOH-d_4) δ 7.73 (d, *J* = 6.8 Hz, 2H), 7.00−6.99 (m, 4H), 6.49 (d, *J* = 8.0 Hz, 2H), 4.01 (s, 2H), 3.72 (m, 2H), 3.15 (m, 2H), 2.19 (s, 3H). *m/z* = 324.2 (M + 1).

Synthesis of ***32***. 2-(4-Fluorophenyl)-3-(*p*-tolylamino)-7,8-dihydroimidazo[1,2-*a*]pyrazin-6(5*H*)-one:

dx.doi.org/10.1021/jm300041e | *J. Med. Chem.* 2012, 55, 4244−4273

Compound **32** was synthesized from compound **7** (R_1 = R_2 = H) $Pd_2(dba)_3$ mediated coupling reaction with *p*-toluidine. ^{1}H NMR (400 MHz, DMSO-d_6) δ 8.55 (s, 1H), 7.77−7.75 (m, 2H), 7.26−7.14 (m, 4H), 7.01−6.95 (m, 2H), 6.53 (m, 1H), 4.53 (m, 2H), 4.22 (m, 2H), 2.17 (s, 3H). *m*/*z* = 337.2 (M + 1).

Synthesis of ***33***. 2-(4-Fluorophenyl)-8,8-dimethyl-3-(*p*-tolylamino)-7,8-dihydroimidazo[1,2-*a*]pyrazin-6(5*H*)-one:

Compound **33a** was prepared from **7** by the following way:

To a stirred solution of compound **7** (390 mg, 1.51 mmol, 1.00 equiv) in dichloromethane (20 mL) was added NBS (0.28 g, 1.00 equiv). The resulting solution was stirred for 2 h at rt. The solid was filtered out, and the mixture was washed with a saturated solution of $Na_2S_2O_3$ and dried over Na_2SO_4. The mixture was concentrated under vacuum. The solids was purified by silica gel chromatography (petroleum ether/EtOAc = 1:2) to result in 432 mg (85%) of the title compound as a white solid. ^{1}H NMR (300 MHz, DMSO-d_6) δ 8.76 (s, 1H), 7.94−7.89 (m, 2H), 7.31−7.25 (m, 2H), 4.57 (s, 2H), 1.56 (s, 6H). *m*/*z* = 338 (M + 1).

Compound **33** was prepared from compound **33a** by a $Pd_2(dba)_3$ mediated amination reaction with *p*-toluidine. ^{1}H NMR (MeOH-d_4, 400 Hz) δ 7.62−7.58 (m, 2H), 7.05 (t, *J* = 8.4 Hz, 2H), 6.92 (d, *J* = 8.4 Hz, 2H), 6.52 (d, *J* = 8.4 Hz, 2H), 4.42 (s, 2H), 2.12 (s, 3H), 1.71 (s, 6H). *m*/*z* = 365.2 (M + 1).

Synthesis of ***34***. 3-(4-Chloro-3-fluorophenylamino)-2-(4-fluorophenyl)-8,8-dimethyl-7,8-dihydro imidazo[1,2-*a*]pyrazin-6(5*H*)-one:

Compound **34** was prepared from compound **7b** by a $Pd_2(dba)_3$ mediated amination reaction with 4-chloro-3-fluoroaniline. ^{1}H NMR (MeOH-d_4, 400 Hz) δ 7.74−7.70 (m, 2H), 7.21 (t, *J* = 8.4 Hz, 1H), 7.08 (m, 2H), 6.49−6.40 (m, 2H), 4.43 (s, 2H), 1.72 (s, 6H). *m*/*z* = 403.1 (M + 1).

Synthesis of ***35***. 2-(4-Fluorophenyl)-8,8-dimethyl-*N*-*p*-tolyl-5,6,7,8-tetrahydroimidazo[1,2-*a*]pyrazin-3-amine:

Compound **35** was prepared from compound **35-1** (shown below and prepared by analogy to compound **9** and using Cbz-glycine) by a $Pd_2(dba)_3$ mediated amination reaction with *p*-toluidine followed by a 6N HCl mediated hydrolysis. ^{1}H NMR (MeOH-d_4, 400 Hz) δ 7.78−7.75 (m, 2H), 7.06−6.97 (m, 4H), 6.56 (d, *J* = 8.4 Hz, 2H), 5.16 (s, NH), 4.33 (t, *J* = 4.8 Hz, 2H), 3.74 (t, *J* = 4.8 Hz, 2H), 2.29 (s, 3H), 1.95 (s, 6H). *m*/*z* = 436.2 (M + 1).

Synthesis of ***36***. *N*,2-Bis(4-fluorophenyl)-8,8-dimethyl-5,6,7,8-tetrahydroimidazo[1,2-*a*]pyrazin-3-amine:

Compound **36** was prepared from compound **35-1** by a $Pd_2(dba)_3$ mediated amination reaction with 4-fluoroaniline followed by a 6N HCl mediated hydrolysis. ^{1}H NMR (400 MHz, MeOH-d_4) δ 7.62−7.58 (m, 2H), 7.12−7.08 (m, 2H), 6.68−6.63 (m, 2H), 6.67 (m, 2H), 4.16 (m, 2H), 3.78 (m, 2H), 1.92 (s, 6H). *m*/*z* = 355.1 (M + 1).

■ ASSOCIATED CONTENT

Supporting Information

In vitro ADME of selected analogues; PAMPA vs Log *P*; Caco-2 (A−B) vs Log *P*; Caco-2 A−B/B−A ratio vs Log *P*; Caco-2 (B−A) vs Log *P*. This material is available free of charge via the Internet at http://pubs.acs.org.

■ AUTHOR INFORMATION

Corresponding Author

*Phone: 858-332-4751. E-mail: akc@gnf.org.

Author Contributions

#Equal contribution to this work

Notes

The authors declare no competing financial interest.

■ ACKNOWLEDGMENTS

This work was supported by a translational research grant (WT078285) from the Wellcome Trust and a grant from the Medicines for Malaria Venture to the Novartis Institute for Tropical Diseases, the Genomics Institute of the Novartis Research Foundation, and the Swiss Tropical Institute

■ REFERENCES

(1) (a) Rottmann, M.; McNamara, C.; Yeung, B. K.; Lee, M. C.; Zou, B.; Russell, B.; Seitz, P.; Plouffe, D. M.; Dharia, N. V.; Tan, J.; Cohen, S. B.; Spencer, K. R.; Gonzalez-Paez, G. E.; Lakshminarayana, S. B.; Goh, A.; Suwanarusk, R.; Jegla, T.; Schmitt, E. K.; Beck, H. P.; Brun, R.; Nosten, F.; Renia, L.; Dartois, V.; Keller, T. H.; Fidock, D. A.; Winzeler, E. A.; Diagana, T. T. Spiroindolones, a potent compound class for the treatment of malaria. *Science* **2010**, *329* (5996), 1175−1180. (b) Wu, T.; Nagle, A. S.; Chatterjee, A. K. Road Towards New Antimalarials—Overview of the Strategies and their Chemical Progress. *Curr. Med. Chem.* **2011**, *18* (6), 853−871.

(2) (a) Noedl, H.; Chanthap, L.; Se, Y.; Socheat, D.; Peou, S.; Schaecher, K.; Srivichai, S.; Teja-Isavadharm, P.; Smith, B.; Jongsakul, K.; Surasri, S.; Fukuda, M. Artemisinin resistance in Cambodia? *Trop. Med. Int. Health* **2007**, *12*, 69−69. (b) Noedl, H.; Se, Y.; Schaecher, K.; Smith, B. L.; Socheat, D.; Fukuda, M. M. Evidence of artemisinin-resistant malaria in western Cambodia. *N. Engl. J. Med.* **2008**, *359* (24), 2619−2620.

(3) Vogel, G. The "do unto others" malaria vaccine. *Science* **2010**, *328* (5980), 847−848.

(4) (a) Deng, X.; Nagle, A.; Wu, T.; Sakata, T.; Henson, K.; Chen, Z.; Kuhen, K.; Plouffe, D.; Winzeler, E.; Adrian, F.; Tuntland, T.; Chang, J.; Simerson, S.; Howard, S.; Ek, J.; Isbell, J.; Tully, D. C.; Chatterjee, A. K.; Gray, N. S. Discovery of novel 1*H*-imidazol-2-yl-pyrimidine-4,6-diamines as potential antimalarials. *Bioorg. Med. Chem. Lett.* **2010**, *20* (14), 4027−4031. (b) Kato, N.; Sakata, T.; Breton, G.; Le Roch, K. G.; Nagle, A.; Andersen, C.; Bursulaya, B.; Henson, K.; Johnson, J.; Kumar, K. A.; Marr, F.; Mason, D.; McNamara, C.; Plouffe, D.; Ramachandran, V.; Spooner, M.; Tuntland, T.; Zhou, Y.; Peters, E. C.; Chatterjee, A.; Schultz, P. G.; Ward, G. E.; Gray, N.; Harper, J.; Winzeler, E. A. Gene expression signatures and small-molecule compounds link a protein kinase to *Plasmodium falciparum* motility. *Nature Chem. Biol.* **2008**, *4* (6), 347−356. (c) Plouffe, D.; Brinker, A.; McNamara, C.; Henson, K.; Kato, N.; Kuhen, K.; Nagle, A.; Adrian, F.; Matzen, J. T.; Anderson, P.; Nam, T. G.; Gray, N. S.; Chatterjee, A.; Janes, J.; Yan, S. F.; Trager, R.; Caldwell, J. S.; Schultz, P. G.; Zhou, Y.; Winzeler, E. A. In silico activity profiling reveals the mechanism of action of antimalarials discovered in a high-throughput screen. *Proc. Natl. Acad. Sci. U.S.A* **2008**, *105* (26), 9059−9064. (d) Wu, T.; Nagle, A.; Sakata, T.; Henson, K.; Borboa, R.; Chen, Z.; Kuhen, K.; Plouffe, D.; Winzeler, E.; Adrian, F.; Tuntland, T.; Chang, J.; Simerson, S.; Howard, S.; Ek, J.; Isbell, J.; Deng, X.; Gray, N. S.; Tully, D. C.; Chatterjee, A. K. Cell-based optimization of novel benzamides as potential antimalarial leads. *Bioorg. Med. Chem. Lett.* **2009**, *19* (24), 6970−6974. (e) Yeung, B. K.; Zou, B.; Rottmann, M.; Lakshminarayana, S. B.; Ang, S. H.; Leong, S. Y.; Tan, J.; Wong, J.; Keller-Maerki, S.; Fischli, C.; Goh, A.; Schmitt, E. K.; Krastel, P.; Francotte, E.; Kuhen, K.; Plouffe, D.; Henson, K.; Wagner, T.; Winzeler, E. A.; Petersen, F.; Brun, R.; Dartois, V.; Diagana, T. T.; Keller, T. H. Spirotetrahydro beta-carbolines (spiroindolones): a new class of potent and orally efficacious compounds for the treatment of malaria. *J. Med. Chem.* **2010**, *53* (14), 5155−5164.

(5) Wu, T. N.; Nagle, A.; Kuhen, K.; Gagaring, K.; Borboa, R.; Francek, C.; Chen, Z.; Plouffe, D.; Goh, A.; Lakshminarayana, S. B.; Wu, J.; Ang, H. Q.; Zeng, P.; Kang, M. L.; Tan, W.; Tan, M.; Ye, N.; Lin, X.; Caldwell, C.; Ek, J.; Skolnik, S.; Liu, F.; Wang, J.; Chang, J.; Li, C.; Hollenbeck, T.; Tuntland, T.; Isbell, J.; Fischli, C.; Brun, R.; Rottmann, M.; Dartois, V.; Keller, T.; Diagana, T.; Winzeler, E.; Glynne, R.; Tully, D. C.; Chatterjee, A. K. Imidazolopiperazines: Hit to Lead Optimization of New Antimalarial Agents . *J. Med. Chem.* **2011**, *54*, 5116−5130.

(6) Kercher, T.; Rao, C.; Bencsik, J. R.; Josey, J. A. Diversification of the three-component coupling of 2-aminoheterocycles, aldehydes, and isonitriles: efficient parallel synthesis of a diverse and druglike library of imidazo- and tetrahydroimidazo[1,2-*d*] heterocycles. *J. Comb. Chem.* **2007**, *9* (6), 1177−1187.

(7) Salvadori, S.; Fiorini, S.; Trapella, C.; Porreca, F.; Davis, P.; Sasaki, Y.; Ambo, A.; Marczak, E. D.; Lazarus, L. H.; Balboni, G. Role of benzimidazole (Bid) in the delta-opioid agonist pseudopeptide H-Dmt-Tic-NH-CH(2)-Bid (UFP-502). *Bioorg. Med. Chem.* **2008**, *16* (6), 3032−3038.
(8) (a) Fidock, D. A.; Rosenthal, P. J.; Croft, S. L.; Brun, R.; Nwaka, S. Antimalarial drug discovery: efficacy models for compound screening. *Nature Rev. Drug Discovery* **2004**, *3* (6), 509−520. (b) Vennerstrom, J. L.; Arbe-Barnes, S.; Brun, R.; Charman, S. A.; Chiu, F. C.; Chollet, J.; Dong, Y.; Dorn, A.; Hunziker, D.; Matile, H.; McIntosh, K.; Padmanilayam, M.; Santo Tomas, J.; Scheurer, C.; Scorneaux, B.; Tang, Y.; Urwyler, H.; Wittlin, S.; Charman, W. N. Identification of an antimalarial synthetic trioxolane drug development candidate. *Nature* **2004**, *430* (7002), 900−904.
(9) Liu, B.; Chang, J.; Gordon, W. P.; Isbell, J.; Zhou, Y.; Tuntland, T. Snapshot PK: a rapid rodent in vivo preclinical screening approach. *Drug Discovery Today* **2008**, *13* (7−8), 360−367.
(10) Trager, W.; Jensen, J. B. Human malaria parasites in continuous culture. *Science* **1976**, *193* (4254), 673−675.
(11) (a) Obach, R. S. Prediction of human clearance of twenty-nine drugs from hepatic microsomal intrinsic clearance data: an examination of in vitro half-life approach and nonspecific binding to microsomes. *Drug Metab. Dispos.* **1999**, *27* (11), 1350−1359. (b) Kalvass, J. C.; Tess, D. A.; Giragossian, C.; Linhares, M. C.; Maurer, T. S. Influence of microsomal concentration on apparent intrinsic clearance: implications for scaling in vitro data. *Drug Metab. Dispos.* **2001**, *29* (10), 1332−1336. (c) Chauret, N.; Gauthier, A.; Nicoll-Griffith, D. A. Effect of common organic solvents on in vitro cytochrome P450-mediated metabolic activities in human liver microsomes. *Drug Metab. Dispos.* **1998**, *26* (1), 1−4. (d) Yan, Z.; Caldwell, G. W. Metabolic assessment in liver microsomes by co-activating cytochrome P450s and UDP-glycosyltransferases. *Eur. J. Drug Metab. Pharmacokinet.* **2003**, *28* (3), 223−232.
(12) (a) Avdeef, A.; Bendels, S.; Di, L.; Faller, B.; Kansy, M.; Sugano, K.; Yamauchi, Y. PAMPA—critical factors for better predictions of absorption. *J. Pharm. Sci.* **2007**, *96* (11), 2893−2909. (b) Avdeef, A. The rise of PAMPA. *Expert Opin. Drug Metab. Toxicol.* **2005**, *1* (2), 325−342.
(13) Balimane, P. V.; Chong, S. Cell culture-based models for intestinal permeability: a critique. *Drug Discovery Today* **2005**, *10* (5), 335−343.
(14) (a) Dubin, A. E.; Nasser, N.; Rohrbacher, J.; Hermans, A. N.; Marrannes, R.; Grantham, C.; Van Rossem, K.; Cik, M.; Chaplan, S. R.; Gallacher, D.; Xu, J.; Guia, A.; Byrne, N. G.; Mathes, C. Identifying modulators of hERG channel activity using the PatchXpress planar patch clamp. *J. Biomol. Screening* **2005**, *10* (2), 168−181. (b) Mathes, C. QPatch: the past, present and future of automated patch clamp. *Expert Opin Ther. Targets* **2006**, *10* (2), 319−327. (c) Zheng, W.; Spencer, R. H.; Kiss, L. High throughput assay technologies for ion channel drug discovery. *Assay Drug Dev. Technol.* **2004**, *2* (5), 543−552.
(15) Franke-Fayard, B.; Trueman, H.; Ramesar, J.; Mendoza, J.; van der Keur, M.; van der Linden, R.; Sinden, R. E.; Waters, A. P.; Janse, C. J. A *Plasmodium berghei* reference line that constitutively expresses GFP at a high level throughout the complete life cycle. *Mol. Biochem. Parasitol.* **2004**, *137* (1), 23−33.